Distribution Agreement

In presenting this thesis as a partial fulfillment of the requirements for a degree from Emory University, I hereby grant to Emory University and its agents the non-exclusive license to archive, make accessible, and display my thesis in whole or in part in all forms of media, now or hereafter now, including display on the World Wide Web. I understand that I may select some access restrictions as part of the online submission of this thesis. I retain all ownership rights to the copyright of the thesis. I also retain the right to use in future works (such as articles or books) all or part of this thesis.

Vishal Reddy Kaila April 18, 2012

Use of a Heterologous Promoter, *mes-4*, and *met-2* to Study *spe-5* function during *C. elegans* Spermatogenesis

by

Vishal Kaila

Dr. Steven W. L'Hernault
Adviser

Department of Biology

Dr. Steven W. L'Hernault

Adviser

Dr. William Kelly

Committee Member

Dr. Guy M. Benian

Committee Member

2012

Use of a Heterologous Promoter, *mes-4*, and *met-2* to Study *spe-5* function during *C. elegans* Spermatogenesis

By

Vishal Reddy Kaila

Dr. Steven W. L'Hernault

Adviser

An abstract of
a thesis submitted to the Faculty of Emory College of Arts and Sciences
of Emory University in partial fulfillment
of the requirements of the degree of
Bachelor of Sciences with Honors

Department of Biology

2012

Abstract

Use of a Heterologous Promoter, *mes-4*, and *met-2* to Study *spe-5* function during *C. elegans* Spermatogenesis

By Vishal Reddy Kaila

Fusion of secretory vesicles with the cell membrane creates a spermatozoan surface needed for successful fertilization in the nematode *Caenorhabditis elegans*. Acidification of sperm-specific secretory vesicles, named fibrous body-membranous organelles (FB-MOs), is vital for proper fusion with the cell membrane. This acidification employs the vacuolar H+ ATPase (V-ATPase) that functions across the membrane of secretory vesicles and we hypothesize that *spe-5*, a gene that encodes a B subunit of the V-ATPase, participates in this process. There are two known paralogs that encode a B subunit of the V-ATPase in *C. elegans*: *spe-5* and *vha-12*. Both genes have similar amino acid sequences (~83%) but have different chromosomal locations. *spe-5* is found on chromosome I and *vha-12* is on the X chromosome, which is silenced during spermatogenesis. Mutants in *spe-5* are sterile and produce no progeny. However, an extrachromosomal array with *vha-12* driven by its own promoter in a *spe-5* mutant displayed a partial rescue of the self-sterile phenotype of this mutant. In this study, *C. elegans spe-5* mutants were crossed into *met-2*, a gene that blocks the germline specific X chromosome silencing seen in *C. elegans* mutants, however the resulting double mutant yielded no progeny. In addition, *met-2* and *mes-4*, another gene that blocks germline specific X chromosome silencing in *C. elegans*, were targeted via RNAi in *spe-5* mutants. While *spe-5* mutants subjected to *met-2* RNAi did not have increased progeny, *spe-5* mutants that had RNAi knockdown of *mes-4* had an increase in the number of progeny. Morphology of sperm in *spe-5* mutants subject to *mes-4* RNAi was affected so that they became similar to wild type sperm. These data suggest that misexpression of *vha-12* in its native location on the X-chromosome can partially compensate for thedefects seen in *spe-5* mutants, presumably by restoring function during *C. elegans* spermatogenesis. In future experiments, *spe-5* mutants containing a copy of *spe-5*, driven by the *vha-12* promoter will be examined to determine transcriptional regulation of *spe-5* during spermatogenesis.

Use of a Heterologous Promoter, *mes-4*, and *met-2* to Study *spe-5* function during *C. elegans* Spermatogenesis

By

Vishal Reddy Kaila

Dr. Steven W. L'Hernault

Adviser

A thesis submitted to the Faculty of Emory College of Arts and Sciences
of Emory University in partial fulfillment
of the requirements of the degree of
Bachelor of Sciences with Honors

Department of Biology

2012

Table of Contents

List of Tables and Figures

Figures

Tables

CHAPTER I

Introduction

A. Overview of *Caenorhabditis elegans*

Described first as a model organism by Sydney Brenner in 1974, *Caenorhabditis elegans* is a transparent soil nematode found throughout the world (BRENNER 1974; RIDDLE and ALBERT 1997). Around one millimeter in length, several characteristics of C. *elegans* make it a powerful model organism in the study of biology. One of the qualities that make C. *elegans* well suited for biological research is the acceptance of the Bristol (N2) strain as a baseline wild-type strain. In comparison, *Drosophila melanogaster* has at least four widely used strains defined as "wild-type" (W1118, Canton S, Oregon R, and Yellow White). The N2 strain possesses a 101 Megabase genome in 5 autosomes labeled I-IV and a single X chromosome. In the laboratory, worms are easily cultured at either 16°C, 20°C or 25°C on agar plates and seeded with drops of an auxotroph strain of *E. coli* known as OP50. When strains deplete the bacteria on a particular plate, a piece of the agar from the depleted plate can be placed onto a freshly seeded agar plate to maintain the strain. Strains can be maintained indefinitely in cryogenic storage (RIDDLE and ALBERT 1997). These qualities allow for the storage of C. *elegans* strains for long periods of time with relative ease.

Populations of nematodes are made up of either XX hermaphrodites, or much less commonly, XO males, which arise due to spontaneous X nondisjunction during meiosis (HERMAN *et al.* 1979). Wild-type worms go through a life cycle of roughly 3.5 days from fertilization to sexual maturation at 25°, although this time period can be extended by several days by culturing the worms at lower temperatures. *C. elegans* goes through four larval stages (designated L1-L4), and will die an average of 2.5 weeks after fertilization (RIDDLE and ALBERT 1997). Wild-type XX hermaphrodites are self-fertile and produce an

average of ~300 progeny. During the L4 stage, a hermaphrodite will produce as many as 350 mature sperm and store them in their spermatheca. Afterwards, the hermaphrodite gonad *switches* to oocyte production and every spermatozoon will fertilize an oocyte (RIDDLE and ALBERT 1997). XO males fertilize hermaphrodites and produce larger sperm that outcompete sperm produced by hermaphrodites, thus increasing genetic diversity in a population. The self-fertility of *C. elegans* hermaphrodite's allows strains to be easily maintained. XO males can be used to produce outcross progeny when doing genetic crosses.

B. Spermatogenesis

Spermatogenesis is the process by which mature, functional sperm are created from an undifferentiated germ cell. Sperm are highly specialized cells that carry a nucleus along with the components needed to successfully fertilize oocytes. Both *C. elegans* hermaphrodites and males engage in spermatogenesis. Hermaphrodites, unlike males, begin spermatogenesis during the L4 larval stage and then switch to oogenesis during the adult stage. *C. elegans* is a spermatogenesis can be readily studied *in vivo* since *C. elegans* worms are transparent. In addition, homogenous sperm can be purified in adequate quantities to allow biochemical analyses (KLASS and HIRSH 1981; NELSON *et al.* 1982).

The development of sperm in *C. elegans* begins with the production of 4N primary spermatocytes from the syncytial rachis (See Figure 1A). These 4N primary spermatocytes then go through the first round of meiosis to produce two 2N secondary spermatocytes. The secondary spermatocytes then go through the second round of meiosis to create two haploid spermatids. The spermatids then bud off a large residual body. Spermatids are loaded with components absolutely required for successful fertilization and the rest is

discarded in the residual body. During spermatogenesis, spermatocytes go through several morphological changes required for entry into spermiogenesis (SHAKES and WARD 1989; WARD *et al.* 1983). One of these changes involves the dispersal of depolymerized Major Sperm Protein (MSP) into each of the four spermatids budding from the residual body. MSP derives from depolymerized fibrous bodies(FB) that are associated with Golgi-derived membranous organelles (MOs) (WARD and KLASS 1982).

C. The Fibrous Body-Membranous Organelle

When spermatids bud from the residual body, all ribosomes are discarded in the residual body. Therefore all proteins required for successful fertilization must be transported into spermatids before they completely separate from the residual body (ROBERTS *et al.* 1986). Fibrous body-membranous organelles (FB-MOs) are required for the transport of proteins required for spermiogenesis (ROBERTS *et al.* 1986). FB-MOs begin their development as part of Golgi complexes in primary spermatocytes still attached to the rachis (WOLF *et al.* 1978).

The structure of FB-MOs is made up of three components. A lobular shaped head region is separated from the body region by an electron-dense collar (WOLF *et al.* 1978). The fibrous body and membranous organelle seem to be two separate structures that are coupled to each other. The head region comes to lie close to the plasma membrane during spermiogenesis (See Figure 1B). The body region employs a double membrane to almost completely surround a fibrous body, which is composed of polymerized MSP (ROBERTS *et al.* 1986).

During spermatogenesis, FB-MOs associate with spermatocytes and later on FB-MOs segregate to spermatids during budding from residual bodies. After a spermatid separates from the residual body, the membrane of the body will fold up to expose the fibrous body to the cytoplasm of the spermatid. Then, the MSP fibers of the fibrous body will depolymerize and spread throughout the cytoplasm (WARD *et al.* 1986). The MOs then move to the membrane and, as spermiogenesis begins, the head region of the MO will fuse with the plasma membrane and exocytose its contents (WOLF *et al.* 1978). The electron dense collar remains embedded in the plasma membrane as a fusion pore. The FB-MO acts to provide the molecular components for sperm to undergo spermiogenesis.

D. Mutations affecting spermatogenesis

Screening for spermatogenesis-defective mutants: C. *elegans* spermatogenesis-defective mutants (classified as either *spe* or *fer*) were readily identified since they alter hermaphrodite self-fertility. Wild type worms lay easily identifiable eggs that are shelled and oval-shaped (WARD and CARREL 1979). On the other hand, spermatogenesis-defective mutants lay unfertilized oocytes, which are characterized by their circular shape and lack of a shell. Isolating *spe* (*spe*rmatogenesis-defective) or *fer* (*fer*tilization-defective) mutants involves mutagenizing hermaphrodites and screening for hermaphrodites that lay large numbers of oocytes. Currently, there are 44 known genes and 90 unassigned mutations that affect various stages of spermatogenesis. These *spe* and *fer* mutants cause a wide range of phenotypes and affect different stages of spermatogenesis (NISHIMURA and L'HERNAULT 2010).

Mutations that affect the FB-MO: There are two classes of mutations that affect FB-MOs: Class I mutants affect FB-MO morphogenesis and class II mutants fail to move FB-MOs

into spermatids. At present, *wee-1.3* is the only cloned class II mutant. *wee-1.3* mutants fail to place FB-MO's into spermatids because they fail to make spermatids. This mutant arrests at the primary spermatocyte stage. See Figure 2 for an overview of these genes.

Class I FB-MO mutations

spe-39: *spe-39* encodes a hydrophilic, cytoplasmic protein that is *not* associated with FB-MOs in both spermatocytes and spermatids. These mutants are characterized by terminal spermatocytes that lack MOs but possess small vesicles with internal membranes, which are reminiscent of what is seen in wild-type MOs. In addition, a double layered membrane does not surround the FB, displaying that the FB can form in the absence of MOs (ZHU and L'HERNAULT 2003). SPE-39 participates in vesicular trafficking to the lysosome in all animal cells. Studies of the *spe-39* gene found that it is a protein involved in vesicular trafficking in all metazoan. These data also suggest that the MO is a modified lysosome (ZHU *et al.* 2009).

spe-6: *spe-6* encodes a casein I type serine threonine kinase (MUHLRAD and WARD 2002). In *spe-6* mutants, the MSP fails to form fibrous bodies (VARKEY *et al.* 1993). As a result, FB-MOs never form and *spe-6* mutants form terminal spermatocytes. This suggests that phosphorylation plays a role in the regulation of FB-MO morphogenesis.

spe-4: *spe-4* encodes a sperm specific presenilin (L'HERNAULT and ARDUENGO 1992). Presenilins are intramembranous aspartyl proteases that process other membrane proteins, such as Alzheimer's precursor protein in the human brain (XIA and WOLFE 2003). Like *spe-39* mutants, *spe-4* mutants produce FBs that are not coupled to MOs, and thus produce terminal spermatocytes. The SPE-4 protein is located in the MO (ARDUENGO *et al.* 1998) .

spe-5: *spe-5* encodes the B subunit of a vacuolar ATPase that is FB-MO specific (GLEASON *et al.* 2012). *spe-5* mutants produce terminal spermatocytes that contain four haploid nuclei. Sporadically, *spe-5* mutants display partial self-fertility, suggesting that some mature sperm still form. The defects seen in *spe-5* mutants are likely due to the lack of FB-MO acidification since V-ATPases acidify vesicular compartments (NISHI and FORGAC 2002).

spe-17: *spe-17* encodes a small soluble protein with no other known homologs outside of nematodes (L'HERNAULT *et al.* 1993). *spe-17* mutants produce FB-MOs that have ribosomes attached to the membrane and, as a result, produce spermatids that contain ribosomes. The FBs can still disperse MSP into the spermatid cytoplasm, but many MOs fail to bind the plasma membrane during spermiogenesis (SHAKES and WARD 1989).

spe-10: *spe-10* encodes a four pass integral membrane protein that localizes to FB-MOs (GLEASON *et al.* 2006). This protein has a DHHC domain, which is an enzyme motif predicted to act as a palmitoyl transferase. In *spe-10* mutants, FB-MOs are produced normally but, during spermatid budding, the membrane surrounding the fibrous body retracts prematurely. As a result, MSP is dispersed throughout the residual body, leaving spermatids deficient in MSP. *spe-10* sperm are immotile and contain MOs that do not fuse with the plasma membrane (SHAKES and WARD 1989). *spe-10,* along with *spe-17,* mutants also produce spermatids that are ~66% the wild type size and have eccentrically placed nuclei (SHAKES and WARD 1989).

fer-6: *fer-6* mutants produce spermatids in which FBs fail to fold back the membrane holding the fibrous body and release MSP. In addition, many MOs fail to fuse with the plasma membrane during spermiogenesis in *fer-6* mutants (WARD *et al.* 1981).

fer-15: *fer-15* mutants produce spermatids that fail to respond to *in vitro* activator, so spermatozoa do not form (S. W. L'Hernault and S. Ward, unpublished).

fer-1: *fer-1* encodes a dysferlin family one pass transmembrane protein. *fer-1* mutants undergo normal FB-MO morphogenesis but the MOs fail to fuse with the membrane and they produce short pseudopods that results in decreased motility (ACHANZAR and WARD 1997; ROBERTS and WARD 1982; WARD *et al.* 1981). FER-1 was the defining member of the "ferlin family" of proteins, consisting of multiple C2 domains and a C- terminal transmembrane domain. Mutations in human dysferlin result in several forms of muscular dystrophy (BASHIR *et al.* 1998). Dysferlin is localized to vesicles at the muscle cell membrane and is likely involved in repairing damaged cell membranes (BANSAL and CAMPBELL 2004).

CHAPTER II

Literature Review of Vacuolar ATPase

My work focuses on the *spe-5* gene, which encodes a B subunit of the V-ATPase. What follows is a brief review of V-ATPase function, which has been extensively analyzed.

A. Overview of V-ATPase

The Vacuolar (H+)- ATPase (V-ATPase) is a membrane bound protein composed of at least 13 different subunits that work together to harness energy from the hydrolysis of ATP to pump protons across membranes (FORGAC 1999; NISHI and FORGAC 2002; STEVENS and FORGAC 1997) (See Figure 3). In comparison, F-ATPase employs a chemical gradient to produce ATP. The V-ATPase, by pumping protons, can create both proton and electrochemical gradients across a membrane that can be used for a number of cellular functions. V-ATPase is found in the membranes of clathrin-coated vesicles, synaptic vesicles, endosomes, storage vesicles, lysosomes and the central vacuole of plants (STEVENS and FORGAC 1997). Two specific roles of V-ATPase in cellular functions are briefly described below.

The endocytic pathway: Endocytosis is the process by which cells engulf extracellular molecules inward folding of the cellular membrane to create small vesicles (GRUENBERG 2001). Endocytosis is often initiated by the binding of ligand-specific receptors on the external surface of the cell. Specialized proteins form membrane invaginations and this allows the vesicle to bud off as an endosome. The contents of the endosome are processed by the acidifying action of V-ATPase, allowing, for instance, ligand-receptor complexes to dissociate. In addition, carrier vesicles that transport endosomal contents between compartments of the endocytotic pathway required acidification provided by V-

ATPases. Therefore, V-ATPases provide the compartmentalized acidic environments necessary for enzymes and other cellular processes to function properly.

Osteoclasts: Living bone is a dynamic structure characterized by the continuous modeling by two different types of cells. Osteoblasts continuously form new bone and osteoclasts degrade bone and the constant balancing of each is required for healthy bone growth. V-ATPases play a crucial role in active osteoclasts. Active osteoclasts are polarized cells with one side of the membrane attaching to bone, and this creates a sealed microenvironment. V-ATPases, along with calcium pumps, pump protons and calcium ions into the microenvironment to lower the pH to ~4.5. This acidic environment promotes the breakdown of bone. V-ATPase is required for proper osteoclast function and the loss of the V-ATPase leads to a significant reduction in bone reabsorption. Consequently, mice lacking an osteoclast specific subunit of V-ATPase often die from osteosclerosis (SCIMECA *et al.* 2000).

B. Structure and function of V-ATPase

V-ATPases are multimeric complexes that function as proton-pumping rotary nano-motors (See Figure 3). The structure of V-ATPases is highly conserved across evolution as yeast and mammalian V-ATPases have a high degree of homology in their subunit compositions as well as biochemical similarities. The cytoplasmic V_1-sector, which is the site of ATP hydrolysis, is composed of eight different subunits with defined stoichiometry ($A_3B_3CDEFG_2H_{1-2}$) (NISHI and FORGAC 2002). The transmembrane V_O-sector, which is

responsible for proton translocation across a membrane, is composed of six different subunits ($ac_4c'c''de$).

The cytoplasmic V_1-sector contains a globular headpiece with three alternating copies of subunits A and B that form a ring (See Figure 3). ATP hydrolysis occurs in this nucleotide binding hexameric domain. There are two genes that encode for the "A" subunit in yeast (KANE 2006). The A subunit has catalytic residues required for the hydrolysis of ATP and has 25% amino acid identity with the β subunit in the F-ATPase (HIRATA *et al.* 1990). The A subunit of the V-ATPase and the β subunit of F-ATPase share a Glu residue that plays a significant role in activating water molecules for the nucleophilic attack of the phosphodiester bond in ATP. The B subunit, which is encoded by both *spe-5* and *vha-12* in C. *elegans,* contains noncatalytic nucleotide-binding residues, and thus it may facilitate nucleotide binding to the A subunit. The B subunit has ~25% amino acid similarity with its homolog in the F-ATPase, the α subunit. Experiments have shown that mutations in the noncatalytic nucleotide binding sites alter V-ATPase activity, providing evidence that the B subunit is necessary for maintaining A subunit activity. Only one isoform of the B subunit exists in S. *cerevisiae,* but in mammals multiple genes express isoforms of the B subunit in a tissue specific manner. They kidney "B1" and brain "B2" isoforms share 90% amino acid identity and 77% mRNA identity (BERNASCONI *et al.* 1990).

The rest of the subunits of the cytoplasmic V_1-sector will be briefly described. It is interesting to note that while the A and B subunits have clearly defined homologs in the F-ATPase, the other components of the V_1-sector, except for subunit G, do not have homologs

with significant similarities in amino acid sequence. The C subunit plays a role in the assembly and dissociation of the V_1 and V_O sectors, as knockouts of the C subunit in yeast leads to the decoupling of the V_1 and V_O sectors. The D subunit, while having no sequence similarity to the γ subunit of F-ATPase, is structurally similar (NELSON *et al.* 1995). Similar to the C subunit, knockouts in the D subunit lead to partial uncoupling of the V_1 and V_O sectors. Therefore, it may function to link ATP hydrolysis to proton transport, possibly in a similar fashion to the γ subunit of F-ATPase. Subunits E, F, G, and H all play a role in the structural integrity of the V-ATPase. Knockouts in the E subunit prevent the assembly of the entire V-ATPase complex (HO *et al.* 1993). Interestingly, evidence suggests that the E subunit also interacts with the B subunit via disulfide linkages, possibly forming part of the peripheral stalk of the V-ATPase (ARATA *et al.* 2002). The F subunit role in V-ATPase structure is unique because although it is part of the V_1-sector, F subunit knockouts lead to disassembly of the V_O-sector (GRAHAM *et al.* 1994). Null mutants of the G subunit leads to failure of V-ATPase assembly (SUPEKOVA *et al.* 1995). The G subunit has been shown to closely associate with the E subunit, and the subunit becomes unstable in the absence of the G subunit. The H subunit is not required for the coupling of the V_1 and V_O sectors, however the V-ATPase formed is nonfunctional and is prone to dissociation of its two sectors (HO *et al.* 1993).

The V_O domain primarily functions to translocate protons, however several V_O subunits play a structural role in the stalks of the two domains of V-ATPase. The V_O domain is made up of single copies of the *a, d, c', and c''* subunits and several copies of the *c* subunit arranged in a ring (NISHI and FORGAC 2002).

The *a* subunit plays a role in proton translocation. It has two isoforms that share 54 percent identity in yeast and 4 isoforms in C. *elegans* (MANOLSON *et al.* 1994; OKA *et al.* 2001; PUJOL *et al.* 2001). The *a* subunit, while not a homolog of the F-ATPase a subunit, plays a similar role as a hydrophilic proton pathway leading to the c subunit. Also, mutations in Arg residues in *a* subunits of both V-ATPases and F-ATPases halt proton translocation (KAWASAKI-NISHI *et al.* 2001b). These experiments suggest that the a subunit acts as a channel that mediates proton interactions with the c subunit. The c, c′, and c′′subunits make up the proteolipid ring that is absolutely required for proton translocation. The subunits share amino acid similarity, and c′ and c′′ have 57% and 29% amino acid similarity with the c subunit, respectively. The subunits cannot replace each other and all play a crucial role in the proteolipid c ring (HIRATA *et al.* 1997; UMEMOTO *et al.* 1991).

There are several proposed proton-translocating mechanisms for V-ATPase. One involves the hydrolysis of ATP causing rotation of the proteolipid c ring. Then the inner half channel of subunit *a* allows cytoplasmic H+ to access and bind to one of the subunits in the c-ring. After a full rotation by the c-ring, H+ unbinds and exits the membrane through the outer half channel of subunit a (MURATA *et al.* 2005).

C. Regulation of V-ATPase activity

Due to its many functions in physiological processes, regulation of V-ATPase is necessary for the cell to avoid both depleting its ATP and over-acidifying vesicles. Regulation of V-ATPase can occur through a variety of mechanisms, including reversible dissociation of the V_1V_O sectors, control the V-ATPase cellular location and changes in the coupling

efficiency of proton transport with ATP hydrolysis (FORGAC 2007). Regulation of V-ATPase via reversible dissociation of the V_1V_O sector and changes in the efficiency of coupling of proton transport with ATP hydrolysis is briefly described below.

Reversible dissociation of V_1V_O sectors: The V_1 and V_O sectors can reversibly dissociate into their separate domains when exposed to various stimuli, which ends proton translocation activity (KANE 2006). This occurs during glucose depletion in yeast and in insects during molting (BEYENBACH and WIECZOREK 2006; KANE 2006). In yeast, V-ATPase dissociation does not require any protein synthesis and is not involved in many of the signal transduction pathways seen in nutrient depleted cells (KANE 2006). V-ATPase simply dissociates into its V_1 and V_0 domains in response to low glucose levels and restoration of glucose levels causes reassembly (KANE 1995). Glucose activity does not, however, directly cause the dissociation of V-ATPase and instead involves a pathway with other proteins, such as aldolase (LU *et al.* 2004). The role of glucose in V-ATPase regulation suggests that cells control V-ATPase activity as a mechanism to conserve energy when starved.

Regulation of V-ATPase coupling efficiency: In lemons, fruit vacuoles have a pH as low as 2.2, while other plant vacuoles are around 5.0-6.5, which shows that V-ATPase-modulated acidification of organelles is precisely regulated (MULLER *et al.* 1997). A possible explanation for different levels of V-ATPase activity is regulation of coupling proton translocation activity to ATP hydrolysis. If a V-ATPase has a reduced coupling efficiency, then fewer protons are transported per ATP hydrolyzed. V-ATPases with different isoforms of subunit *a* have different coupling efficiencies, due to differences in the *a* subunit C terminal amino acid sequences (KAWASAKI-NISHI *et al.* 2001a; KAWASAKI-NISHI *et al.* 2001b).

Furthermore, mutations in both subunit d and subunit A increase coupling efficiency, which suggests that wild-type V-ATPase is not fully optimized for proton translocation activity (OWEGI *et al.* 2006; SHAO *et al.* 2003). Thus, V-ATPase can be regulated via coupling efficiency to either increase or decrease proton translocation activity.

D. V-ATPase and vesicular trafficking

The V-ATPase and its function to acidify organelles also play a role in vesicular trafficking. Exocytosis of insulin-containing secretory vesicles in mediated, at least in part, by the V-ATPase. Mouse Null mutants of the a3 V-ATPase do not show insulin release after exposure to glucose or membrane depolarization. Interestingly, inhibition of the V-ATPase with bafilomycin, which prevents proton translocation, does not prevent insulin release in normal mice, suggesting that the V-ATPase might play a role in vesicles that does not relate directly to acidification (SUN-WADA *et al.* 2007). While V-ATPase roles in the endocytic pathway was already addressed, various toxic molecules, viruses, and bacteria alter V-ATPase to improve propagation of disease. For example, *Mycobacterium tuberculosis* inhibits V-ATPase, causing the acidity of phagosomes to be reduced, which impairs their fusion with lysosomes (HUYNH and GRINSTEIN 2007).

Outside of the exocytic and endocytic pathways, V-ATPases mutants have various defects in vesicular trafficking. Deletion of the mouse c-subunit causes weakened acidification and defective intracellular trafficking that is required for proper development. There are numerous other instances in several organisms where knockouts in various V-ATPase subunits have led to altered vesicular trafficking. The a subunit in C. *elegans* has

been linked to the secretion of *Hedgehog*-related proteins from exosome to the apical membrane (LIEGEOIS *et al.* 2006). The V_O a subunit in *Drosophila melanogaster* is involved in synaptic cell fusion in neurons (HIESINGER *et al.* 2005). Together, these data provide evidence that the V-ATPase plays a significant role in vesicular trafficking and other cellular processes.

CHAPTER III

Germ-line silencing of the X chromosome in *C. elegans*

A. Overview

In the germ line of C. *elegans*, the X chromosomes of XX C. *elegans* hermaphrodites are globally silenced during early germ cell development and during all stages of XO males (KELLY *et al.* 2002). The X chromosomes are under populated with genes required for germ cell development, especially genes involved with spermatogenesis; there are no examples of *spe* genes that are located on the X chromosome (S. W. L'Hernault, personal communication). MES proteins participate in the silencing of the X chromosome in XX animals and MET proteins mediate the inactivation of the X chromosome in XO animals (CHECCHI and ENGEBRECHT 2011; FONG *et al.* 2002).

It is thought that this global silencing process of C. *elegans* X chromosomes arose as a defense mechanism against the lack of a pairing partner for the male X chromosome during meiotic segregation (KELLY *et al.* 2002). Genes required for spermatogenesis are, as well as other germ-line expressed genes, underrepresented on the X chromosome (REINKE *et al.* 2004; REINKE *et al.* 2000). X/autosome paralogs exist where the autosomal copy of the gene is expressed in the germ-line. Genes on the X chromosome will function in somatic cells except in germ cells, where the autosomal copy of the gene will be active (MACIEJOWSKI *et al.* 2005).

B. X- chromosome silencing in the germ line

Mechanisms to silence the X chromosome in the germ line of C. *elegans* are intrinsically different than the regulation of the X- chromosome seen in dosage compensation complex (DCC) mechanisms. Interestingly, DCC is completely absent in the

germ line, suggesting that there are other mechanisms to down-regulate the X-chromosome. Presently, experiments have shown that the X chromosome of both XX and XO animals are completely silenced (KELLY *et al.* 2002). The silencing seen in XX animals is characterized by histone post translational modifications that include H3K27 methylation along with the absence of histone acetylation (BENDER *et al.* 2004a; KELLY *et al.* 2002).

C. XO male heterochromatin dynamics

The transcriptional silencing of the X chromosome in male *C. elegans* is similar to that of transcriptional silencing of the X chromosome in male mammals. During meiotic prophase, the X chromosome in males prematurely condenses. Likewise, the X and Y chromosomes in mammals hypercondense into a "sex body" that is transcriptionally silent (HANDEL 2004). This premature X chromosome condensation is also seen during sperm meiosis in XX hermaphrodites and is not seen, however, in germ cells involved in oogenesis.

Another distinct feature of XO males is the enrichment of the histone modification H3K9me2 (KELLY *et al.* 2002). This enrichment does not occur during XX hermaphrodite spermatogenesis or sexually transformed XX male spermatogenesis, suggesting that the lack of a second X chromosome leads to H3K9me2 enrichment. In C. *elegans*, MET-2 is the histone methyltransferase, and it is required for all H3K9me2 deposition in the adult germ line (CHECCHI and ENGEBRECHT 2011).

D. MES histone modifiers

C. *elegans* proteins MES-2, MES-3, MES-4, and MES-6 are involved in the global silencing of the X-chromosome. Null mutations in any of the *mes* genes results in defects of

germ cell proliferation, necrotic degeneration of germ cells and maternal-effect sterility (CAPOWSKI *et al.* 1991; GARVIN *et al.* 1998). *mes* mutant XX worms are more severely affected than XO animals, suggesting that MES proteins are implicated primarily in XX animals (GARVIN *et al.* 1998). Also, while the germ cells of wild-type hermaphrodites lack histone acetylation as described previously, *mes* mutants show histone post translational modifications that usually mark an active chromosome (FONG *et al.* 2002; KELLY *et al.* 2002).

MES-2, MES-3, and MES-6 form a complex to possibly mediate X-chromosome silencing (KETEL *et al.* 2005; XU *et al.* 2001). The MES complex has the orthologs E(Z) in flies and EZH2 in vertebrates and accounts for all H3K27 methylation in most areas of both the germ line and the early embryo (BENDER *et al.* 2004b; KETEL *et al.* 2005). MES-2, which possesses a SET domain, is a histone methyltransferase (HMT) and it is catalytically active on H3K27 (BENDER *et al.* 2004b). MES-2 requires association with both MES-3 and MES-6 in order to show HMT activity (KETEL *et al.* 2005).

While the MES-2/MES-3/MES-6 complex directly acts on the X chromosome to repress gene expression, MES-4 is involved with the silencing of the X-chromosome while almost exclusively associating with the autosomes (BENDER *et al.* 2006; FONG *et al.* 2002). Loss of MES-4 leads to ~1.8 fold increase in X- chromosome compared to wild-type worms (BENDER *et al.* 2006). MES-4 is required for H3K36me2 activity in the germ line as well as early embryos while other HMTs are responsible for H2K36 methylation in somatic tissue and later stage tissues. Thus, it is hypothesized that MES-4 methylation plays a germ-line epigenetic role rather than a transcription based role (BENDER *et al.* 2006). A possible

mechanism for MES-4 mediated X-chromosome silencing is that MES-4 focuses repressor action on the X chromosome (FONG *et al.* 2002).

CHAPTER IV

Factors that Control V-ATPase B subunit Expression during *C. elegans* Spermatogenesis

A. Introduction to SPE-5

The development of mature spermatozoa in *C. elegans* is characterized by the acidification of fibrous body-membranous organelles (FB-MOs) (HILL 2000). These FB-MOs fuse with the cell surface and this fusion is required for the sperm to become competent for fertilization (L'HERNAULT 2006). The FB-MOs are acidified by the V-ATPase, which uses the energy from ATP hydrolysis to drive protons into the FB-MO against a pH gradient (GLEASON *et al.* 2012). The V-ATPase is highly conserved in eukaryotes and contains 14 different polypeptides (FORGAC 2007). The distinguishing characteristics between different V-ATPases are linked to the nature of the "a" subunit in some species. For instance, there are two genes that encode for the "a" subunit in yeast (KANE 2006). In humans and other animals, several subunits are found to have more than one gene encoding for it (FORGAC 2007). This suggests that V-ATPases can be optimized for a particular function.

The B subunit, which participates in ATP hydrolysis, has two paralogs in *C. elegans*. *C. elegans* mutants with a loss of function mutation in *spe-5*, which encodes one of these two B subunits (GLEASON *et al.* 2012) are found to be self-sterile due to defective FB-MOs (MACHACA and L'HERNAULT 1997). Immunostaining with specific antibodies for *spe-5* revealed localization of *spe-5* in the FB-MOs(GLEASON *et al.* 2012). The gene that encodes the other paralog, *vha-12* (~83% similarity in amino acid sequence) is found on the X-chromosome. Presumably, *vha-12* is transcriptionally silent as is the case for other genes on the X-chromosome during spermatogenesis (KELLY *et al.* 2002), but an extrachromosomal array with *vha-12* driven by its own promoter allows partial rescue of the *spe-5* phenotype (GLEASON *et al.* 2012). Therefore we hypothesize that the autosomal location of *spe-5* on

chromosome I evolved to allow expression of a B subunit during spermatogenesis. I analyzed *spe-5* gene activity in *spe-5* mutants with a transcriptionally active X chromosome. This was accomplished using *met-2* and *mes-4,* genes that control X-chromosome silencing in C. *elegans* (BENDER *et al.* 2006; CHECCHI and ENGEBRECHT 2011; KELLY and FIRE 1998). *met-2* and *mes-4* were targeted via RNAi and genetic approaches in *spe-5* mutants. This hypothesis will also be tested by creating a *C. elegans* mutant containing a *spe-5* coding sequence driven by the *vha-12* promoter in an extrachromosomal array.

B. Materials and Methods

In order to transcriptionally activate the X-chromosome during spermatogenesis, *met-2* was crossed into *spe-5* mutants. *met-2* and *mes-4* were also knocked down via RNAi. A total of 26 *spe-5* mutant hermaphrodites were exposed to *met-2* and *mes-4* RNAi constructs, in addition to a "blank" pPD129.36 control.

Strains, culture and nomenclature

C. elegans var. Bristol (N2) (BRENNER 1974) was the wild-type strain used for most experiments and the *spe-5* deletion allele (*ok1054*) was provided by the C. *elegans* Knockout Consortium (http://celeganskoconsortium.omrf.org/). *spe-5(ok1054)* mutants lack the *spe-5* start codon, the first two exons and introns along with part of exon three (GLEASON *et al.* 2012). Culturing, manipulation, and genetic analyses were performed as described (BRENNER 1974) except as noted, and standard *C. elegans* nomenclature was used (HORVITZ *et al.* 1979). The *dpy-5(e61)*I (BRENNER 1974), *him-5(e1490)*V (HODGKIN et al. 1979), and *unc-32(e189)III* (BRENNER 1974) mutations were used. *spe-5(ok1054) dpy-5(e61)* double mutants

were maintained as lines with the balancer chromosome *sDp2,* which covers both *spe-5* and *dpy-5* (Howell et al. 1987) and a HA-tagged transgene that expresses *spe-5* in its operon with a *myo-3* gfp transformation marker. *met-2* mutants were provided by the Kelly lab (Emory University).

met-2 cross into _spe-5_ mutants

C. elegans met-2, which is located on chromosome III, has a mutant phenotype that is not easily distinguishable from wild type. Therefore, *spe-5* mutants were first crossed into *unc-32* mutants, also located on chromosome III, so *met-2* could be followed during strain creation (See Figure 9). Twelve mating plates were prepared with 12 *ebEX* balanced *spe-5* mutant males and 4 *unc-32* hermaphrodites at 20°C. The resulting progeny were then allowed to self to yield *spe-5 dpy-5*; *unc-32* double mutants. *met-2* spontaneous males were found by screening several plates of *met-2* mutants and were maintained by creating crosses between *met-2* males and hermaphrodites. *met-2* males and *spe-5 dpy-5*; *unc-32* hermaphrodites were crossed to yield *spe-5 dpy-5 I*; *met2 III* mutants. This cross was done with the HA-tagged transgene (*ebEX*) balanced *spe-5(ok1054)* lines. Progeny counts were assessed by transferring mutant hermaphrodites daily and counting offspring until worms stopped laying.

RNAi Analysis

Vectors

Three RNAi constructs in the pPD129.36, or L4440, plasmid backbone were used to knock down expression of *met-2* and *mes-4* in *spe-5* mutants. The *met-2* and *mes-4* RNAi constructs were obtained from an available RNAi library in HT115 bacteria (KAMATH *et al.*

2003). The constructs were purified and sequenced to confirm the presence of the dsRNA construct using published primers. The pPD129.36blank vector that was used as a negative control was provided by the Benian Lab (Emory University).

Preparation of feeding *E. coli* with RNAi vectors

The *met-2*, *mes-4* RNAi and pPD129.36control constructs were transformed into HT115 *E. coli* bacteria (provided by Kelly and Benian Labs). The resulting bacteria were then cultured overnight and 30 µL of the overnight culture was grown for two hours until the optical density was ~0.4. Isopropyl β-D-1-thiogalactopyranoside(IPTG) was then added to induce the bacteriophage T7 promoter for four hours. The induced cultures were then spotted onto NGM/Amp/Tet/IPTG plates (3g NaCl + 17g agar + 2.5g Bacto-peptone in 1L dH_20, made 100 µg/ml ampicillin, 10 µg/ml tetracycline and 1 mM IPTG). Single *spe-5* mutants were placed on separate plates after allowing the plates to dry. Since *met-2* is a maternal effect gene, *spe-5* mutant lines (balanced with *sDp2*) were fed HT115 transformed with *met- 2* and the resulting offspring were used in counting experiments (CHECCHI and ENGEBRECHT 2011). Due to the fact *mes-4* homozygous mutants produce progeny without a functional germline (*grandchildless* phenotype), these progeny do not produce offspring (BENDER *et al.* 2006). Therefore, *sDp2* balanced *spe-5* mutants were allowed to lay eggs on *mes-4* RNAi feeding plates for 8 hours and were then removed so that the eggs laid would not contain *mes-4* dsRNA. As a result, the eggs laid were still loaded with *mes-4* messenger RNA and the resulting progeny could be used in *mes-4* knockdown experiments. The resulting offspring were then counted once they grew to at least L3 stage. The *spe-5*

mutants in these RNAi feeding studies were transferred ~48 hours since RNAi slowly loses its effect as the IPTG used to induce HT115 slowly degrades over time.

Sperm cytological analyses

spe-5 mutant males were plated in either *mes-4* or *met-2* RNAi plates and were allowed to grow for several days. They were then dissected in 1X sperm medium and analyzed with LysoSensor Blue DND-192 and TEA, for detection of acidification of FB-MOs and sperm activation, respectively (GLEASON *et al.* 2012).

Construct containing *spe-5* driven by *vha-12* promoter

In order for *spe-5* to be driven by the *vha-12* promoter, *spe-5* was cloned into a modified pRW05 plasmid. pRW05 (R. Weimer and E. Jorgensen, University of Utah, personal communication) is a plasmid with a LITMUS 28 vector backbone(New England Biolabs, Ipswich, MA) containing the *vha-12* coding as well as 5' and 3' flanking regions. It has 3,029 base-pairs (bp) upstream of the *vha-12* start codon, the entire *vha-12* coding sequence and a 3' 1,515 bp untranslated region (UTR) of the predicted *vha-12* transcript. The LITMUS 28 vector has the β-lactamase gene that allows bacteria to be resistant to ampicillin. This becomes useful when transforming this vector in bacteria. The *spe-5* sequence was cloned into pRW05 in place of the *vha-12* coding sequence by inserting restriction enzyme recognition sites for *Xma* I directly upstream and downstream of *spe-5* and in place of *vha-12* in pRW05 via site directed mutations (See Figure 4) to allow swapping of the coding sequences.

Insertion of *Xma* I recognition sites in place of of *vha-12*

Using multiple rounds of PCR and primers to *vha-12* and *Xma* I recognition sites, two segments containing an *Xma* I recognition sites and parts of the promoter and 3' UTR in pRW05 were created. The upstream segment (5' of *vha-12*) contained parts of both the promoter region and *vha-12* and the downstream segment (3' of *vha-12*) contained a portion of *vha-12* and the 3' UTR (See Figure 5A). These segments were then subjected to another round of PCR to create a DNA segment containing parts of the *vha-12* promoter and 3' UTR along with an *Xma I* site in between (See Figure 5B). The resulting PCR product was then ligated into pRW05 after restriction digest (See Figure 5C). All of the PCR in this set of experiments was accomplished using the Phusion DNA polymerase kit (New England Biolabs, Ipswich, MA). Ligations were completed with T4 DNA ligase and transformations were done into DH5α competent cells prepared by Eric Brown and Heather Comstra.

Insertion of *Xma I* recognition sites upstream and downstream of *spe-5*

spe-5 is the 3' most gene in the three gene CEOP1216 operon. pMH1 contains this operon in a pBluescript plasmid vector (Stratagene, La Jolla, California). The CEOP1216 operon along with 5' and 3' flanking regions from fosmid 0636 (Geneservice, Cambridge, MA) was inserted into pBluescript via restriction digestion and subsequent ligation.

PCR was again used to insert *Xma* I recognition sites upstream and downstream of *spe-5* in BS-0636 using primers with *Xma* I recognition sites and specific annealing sequences (See Figure 6). After several attempts, the PCR yielded products that did not have the correct sequence. Many of the reactions had non-specific binding of primers that led to multiple PCR products. After ligation and transformation with these PCR products, the plasmids produced did not follow the expected band pattern after gel electrophoresis (See

Table 1). New primers with sequences that had a higher Tm were ordered and the PCR product produced in this reaction had the correct size (See Table 1). This PCR product was then treated with Taq Polymerase (Fisher Scientific, Pittburgh, PA) to add 5' adenosine overhangs to the PCR product. The *spe-5* segment containing *Xma* I sites on both ends was then ligated into the PCR2.1 vector using T4 DNA ligase and then transformed with NEB High Competency DH5α cells (New England Biolabs, Ipswich, MA). The resulting plasmid was then sequenced (UC Berkeley Sequencing Facility) to check for mutations that could have occurred during PCR. The resulting segment was then cut out of PCR2.1 with *Xma* I, purified from an agarose gel, ligated into pVK8 and then transformed with NEB DH5α cells (See Figure 7). The resulting plasmids did not result in a construct with pRW05 and 1 *spe-5* coding sequence in place of the *vha-12* coding sequence. Instead there were *two spe-5* coding sequences in place of *vha-12* (See Figure 8A). Parts of each *spe-5* sequence were then cut out to yield one coding sequence (See Figure 8B).

C. Results

RNAi knockdown of *mes-4* increases brood size in *spe-5* mutants

Previous experiments have shown that *vha-12* in an extrachromosomal array can partially substitute for *spe-5* to encode the V-ATPase during spermatogenesis (GLEASON *et al.* 2012). To test these further, *spe-5* mutants were subjected to RNAi knockdown of genes that would allow for the misexpression of *VHA-12* on the X- chromosome during spermatogenesis. Genes that control X chromosome inactivation were targeted via RNAi since this chromosome is epigenetically silenced during spermatogenesis (KELLY *et al.* 2002).

mes-4 participates in the silencing of the X-chromosome and loss of MES-4 leads to derepression of X-linked genes in the germ line (BENDER *et al.* 2006). Knockdown of *mes-4* via RNAi in *spe-5(ok1054)* mutants leads to elevated self-fertility (mean brood size=39 +/- 6, n=26) compared to *spe-5(ok1054)* mutants treated with L4440 blank vector (mean brood size=11 +/- 2, n=26) (See Figure 10). This elevated self-fertility is roughly half of *dpy-5* controls. Since L4440 controls had elevated self-fertility previously unseen, the *mes-4* RNAi experiment was redone with a *spe-5 dpy-5*; *him-5* line known for being completely self-sterile. Markedly similar results were seen with *mes-4* via RNAi in *spe-5(ok1054)* mutants leading to elevated self-fertility (mean brood size=26 +/- 7.5, n=19) compared to *spe-5(ok1054)* mutants treated with L4440 blank vector (mean brood size=10 +/- 3, n=24) (See Figure 10). Thus, feeding HT115 to *spe-5(ok1054)* mutants leads to elevated self-fertility for unknown reasons. Nevertheless, RNAi knockdown of *mes-4* in both lines increases self-fertility in *spe-5* mutants when compared to the L4440 control.

RNAi knockdown of *mes-4* increases the number of mature sperm in *spe-5* mutants

The development of mature spermatozoa in *C. elegans* is characterized by the acidification of fibrous body-membranous organelles (FB-MOs) (HILL 2000). Wild type spermatids stained with LysoSensor Blue DND-192 show a distinct pattern with bright dots close to the membrane of the spermatids (See Figure 13B). *spe-5* mutants often produce terminal spermatocytes (See 13D) and do not have an acidified FB-MO staining pattern (GLEASON *et al.* 2012). *spe-5* mutants with *mes-4* knocked down via RNAi displayed an increase in the number of sperm, however these sperm do not obviously show acidified FB-MO's when stained with LysoSensor Blue DND-192 (See Figure 14 B, E). While FB-MO's did

not reveal acidified compartments with LysoSensor staining, *spe-5* mutants with RNAi knock down of *mes-4* showed an elevated number of sperm and improved sperm morphology as compared to the non RNAi control *spe-5* mutants. Exposure of the *mes-4* RNAi treated sperm to TEA lead to partial activation of sperm (See Figure 14 C). These *mes-4* RNAi sperm, interestingly, sharing striking similarities in size and morphology of sperm seen in *spe-5(hc93)* mutants. *spe-5(hc93)* mutants are often self-sterile but sometimes have brood sizes of ~40 (MACHACA and L'HERNAULT 1997). These irregular brood sizes are collectively known as the "bursting" phenotype.

***met-2* does not increase brood size in hermaphrodites**

MET-2 participates in X chromosome inactivation in *C. elegans* males as a mechanism to shield it from meiotic checkpoints and chromosome segregation (CHECCHI and ENGEBRECHT 2011). Therefore, loss of *met-2* in *C. elegans* hermaphrodites should lead to desilencing of the X chromosome during spermatogenesis. If X chromosome silencing in hermaphrodites is not prevented, *vha-12* cannot express its B subunit paralog that is needed to replace what is missing in *spe-5* mutants. The brood sizes of *spe-5 met-2* double mutant hermaphrodites were not significantly larger than *spe-5* mutants (See Figure 12). In addition, *spe-5* mutants subjected to RNAi knockdown of *met-2* did not show increased self-fertility (see Figure 10).

***met-2* increases the number of mature sperm in *spe-5* mutant males**

While loss of MET-2 did not lead to increased self-fertility in hermaphrodites, it did lead to increased numbers of mature sperm in males. Dissected male gonads released spermatids, which are not normally seen in *spe-5* mutants (see Figure 14F). LysoSensor DND

192 staining revealed no evidence suggestive of acidified FB-MOs. Sperm were also observed with “pock marks”, which is very common in *spe-5* mutant spermatocytes (see Figure 14F). Thus, while *met-2* knockdown via RNAi did show increased numbers of mature sperm, it did not result in FB-MO acidification or increased fertility.

pVK7 injection and subsequent cross into *spe-5* mutants

pVK7 was finished in March 2011 and injections to create an extrachromosomal array in C. *elegans* have, thus far, been unsuccessful. Attempts to create an extrachromosomal array with *spe-5* driven by the *vha-12* promoter will be continued to see whether VHA-12 can fully substitute for SPE-5 during C. *elegans* spermatogenesis.

D. Discussion

The acidification of FB-MO’s and their subsequent fusion with the cell surface during *C. elegans* spermatogenesis is required for fertilization. Experiments have shown that the acidification seen in FB-MO’s requires V-ATPases that hydrolyze ATP to drive protons into the MO secretory vesicles (GLEASON *et al.* 2012). While *spe-5* normally encodes the B subunit of the V-ATPase, there is evidence that the *vha-12* B-subunit can replace the *spe-5* B subunit in *spe-5* mutants. *spe-5* null mutants, normally completely self-sterile, occasionally produce self-sterile progeny. One of the reasons that may account for self-fertility seen in a few *spe-5* mutants is the misexpression of *vha-12*, a *spe-5* paralog. We hypothesize that *spe-5*’s autosomal location on chromosome I and its ~15 amino acid difference from VHA-12 arose to encode a specialized B-subunit optimized specifically for spermatogenesis.

Previous experiments have shown *vha-12* can partially substitute for *spe-5* to encode the B subunit of V-ATPase during spermatogenesis. These experiments were accomplished using an extrachromosomal array with *vha-12* coding sequence along with its 5' and 3' flanking regulatory sequences (GLEASON *et al.* 2012). *vha-12*'s location on an extrachromosomal array allows it to escape X chromosome silencing. These transgenic *spe-5* mutants have elevated self-fertility with ~36% brood size of control worms (GLEASON *et al.* 2012).

Experiments that allow for the expression of *vha-12* from its native location on the X chromosome are useful in several ways. It provides insight into the specific mechanisms behind the *vha-12* misexpression and it shows that paralogs located on different chromosomes can substitute for each other. Several candidate genes involved with X chromosome inactivation were chosen and knockdown of these genes were analyzed for their effect on *spe-5* mutants. *mes-4* knockdown with RNAi, which desilences genes on the X-chromosome in the C. *elegans* germline (BENDER *et al.* 2006), increases self-fertility in *spe-5* mutants. They also show improved sperm morphology but show little if any acidification of FB-MO's seen in wild type sperm and only partial activation of sperm via TEA. This could be explained by the reduced role of MES proteins in C. *elegans* males (BENDER *et al.* 2006), from which the sperm used for LysoSensor staining were obtained. Future experiments will stain hermaphrodite sperm with LysoSensor would provide further insight into the acidification of FB-MO's in *spe-5* mutants fed *mes-4* dsRNA. Another reason that could explain the lack of FB-MO's acidification in *mes-4* RNAi worms is that *vha-12* misexpression may allow for spermatid budding and subsequent formation of mature sperm, but it does

not successfully acidify FB-MO's to the extent of the B subunit encode by *spe-5*. Others have shown that V-ATPase mediated vesicular trafficking does not necessarily require V-ATPase proton pumping activity (SUN-WADA *et al.* 2007). This suggests that *spe-5* is "specialized" to express the B subunit of V-ATPase during spermatogenesis. This is also supported by *mes-4* RNAi treated sperm being similar to sperm seen in *spe-5(hc93)* mutants, which is known to "burst" (MACHACA and L'HERNAULT 1997).

met-2 also participates in X chromosome silencing via H3K9me2 methylation (CHECCHI and ENGEBRECHT 2011). However, both *spe-5 met-2* double mutants and *spe-5* mutants with RNAi knockdown of *met-2* did not show increased self-fertility in hermaphrodites. A possible reason for this result could be due to the fact that H3K9me2 is primarily enriched on male X chromosomes (BESSLER *et al.* 2010). *spe-5* mutant males with *met-2* knockdown via RNAi displayed increased numbers of mature sperm (See Figures 14 E, F). Thus, analyzing *vha-12* activity in *spe-5* mutants would have to be primarily focused on spermatogenesis occurring in males. Future experiments should subject *spe-5 him-8* double mutants to *met-2* knockdown with either a genetic or RNAi approach since *him-8* mutants have H3K9me2 methylation (BESSLER *et al.* 2010).

The construct containing the *spe-5* coding sequence with a 5' *vha-12* promoter sequence (pVK7) was finished in March 2011. This construct will be microinjected into wild-type *C. elegans* with a visible marker and then crossed into *spe-5* and *spe-5 vha-12* double mutants. A full rescue of V-ATPase B subunit function during spermatogenesis will demonstrate that the *spe-5* encoded B-subunit is sufficient for acidification of FB-MOs during spermatogenesis plus all other tissues. This will mean that the *vha-12* promoter is

capable of properly driving *spe-5* expression during spermatogenesis, but only when it is in an extrachromosomal array. Should this work as planned, this will be the first case of a heterologous promoter working in the *C. elegans* testes to drive a sperm-expressed gene and simplify control of *spe-5* expression, which normally resides in a three-gene operon.

E. Future Directions

- Microinjection of pVK7 into *C. elegans* and subsequent crosses into *spe-5* mutants and evaluation of the nature of phenotypic rescue.
- Immunostaining with SPE-5 antibodies to observe location of *vha-12* driven *spe-5* within *C. elegans* after microinjection with pVK7.
- Crossing *spe-5* mutants into *mes-4* mutants and observing progeny
- Lysosensor staining of *spe-5 mes-4* double mutant sperm collected from hermaphrodites.
- Immunostaining with VHA-12 antibodies to observe expression of VHA-12 in sperm of *spe-5; mes-4* double mutants.
- Replacing *vha-12* in *spe-5*'s native operon and observing differences in brood size along with sperm morphology

References

ACHANZAR, W. E., and S. WARD, 1997 A nematode gene required for sperm vesicle fusion. J. Cell Sci. **110:** 1073-1081.

ARATA, Y., J. D. BALEJA and M. FORGAC, 2002 Cysteine-directed cross-linking to subunit B suggests that subunit E forms part of the peripheral stalk of the vacuolar H+-ATPase. J Biol Chem **277:** 3357-3363.

ARDUENGO, P. M., O. K. APPLEBERRY, P. CHUANG and S. W. L'HERNAULT, 1998 The presenilin protein family member SPE-4 localizes to an ER/Golgi derived organelle and is required for proper cytoplasmic partitioning during *Caenorhabditis elegans* spermatogenesis. J Cell Sci **111:** 3645-3654.

BANSAL, D., and K. P. CAMPBELL, 2004 Dysferlin and the plasma membrane repair in muscular dystrophy. Trends Cell Biol **14:** 206-213.

BASHIR, R., S. BRITTON, T. STRACHAN, S. KEERS, E. VAFIADAKI *et al.*, 1998 A gene related to *Caenorhabditis elegans* spermatogenesis factor *fer-1* is mutated in limb-girdle muscular dystrophy type 2B. Nat Genet **20:** 37-42.

BENDER, A. M., O. WELLS and D. S. FAY, 2004a *lin-35*/*Rb* and *xnp-1*/ATR-X function redundantly to control somatic gonad development in *C. elegans*. Developmental Biology **273:** 335-349.

BENDER, L. B., R. CAO, Y. ZHANG and S. STROME, 2004b The MES-2/MES-3/MES-6 complex and regulation of histone H3 methylation in *C. elegans*. Curr Biol **14:** 1639-1643.

BENDER, L. B., J. SUH, C. R. CARROLL, Y. FONG, I. M. FINGERMAN *et al.*, 2006 MES-4: an autosome-associated histone methyltransferase that participates in silencing the X chromosomes in the *C. elegans* germ line. Development **133:** 3907-3917.

BERNASCONI, P., T. RAUSCH, I. STRUVE, L. MORGAN and L. TAIZ, 1990 An mRNA from human brain encodes an isoform of the B subunit of the vacuolar H(+)-ATPase. J Biol Chem **265:** 17428-17431.

BESSLER, J. B., E. C. ANDERSEN and A. M. VILLENEUVE, 2010 Differential localization and independent acquisition of the H3K9me2 and H3K9me3 chromatin modifications in the *Caenorhabditis elegans* adult germ line. PLoS Genet **6:** e1000830.

BEYENBACH, K. W., and H. WIECZOREK, 2006 The V-type H+ ATPase: molecular structure and function, physiological roles and regulation. J Exp Biol **209:** 577-589.

BRENNER, S., 1974 The genetics of *Caenorhabditis elegans*. Genetics **77:** 71-94.

CAPOWSKI, E. E., P. MARTIN, C. GARVIN and S. STROME, 1991 Identification of grandchildless loci whose products are required for normal germ-line development in the nematode *Caenorhabditis elegans*. Genetics **129:** 1061-1072.

CHECCHI, P. M., and J. ENGEBRECHT, 2011 *Caenorhabditis elegans* histone methyltransferase MET-2 shields the male X chromosome from checkpoint machinery and mediates meiotic sex chromosome inactivation. PLoS Genet **7:** e1002267.

FONG, Y., L. BENDER, W. WANG and S. STROME, 2002 Regulation of the different chromatin states of autosomes and X chromosomes in the germ line of *C. elegans*. Science **296:** 2235-2238.

FORGAC, M., 1999 Structure and properties of the vacuolar (H+)-ATPases. J Biol Chem **274:** 12951-12954.

FORGAC, M., 2007 Vacuolar ATPases: rotary proton pumps in physiology and pathophysiology. Nat Rev Mol Cell Biol **8:** 917-929.

GARVIN, C., R. HOLDEMAN and S. STROME, 1998 The phenotype of *mes-2, mes-3, mes-4* and *mes-6*, maternal-effect genes required for survival of the germline in *Caenorhabditis elegans*, is sensitive to chromosome dosage. Genetics **148:** 167-185.

GLEASON, E. J., P. D. HARTLEY, M. HENDERSON, K. L. HILL-HARFE, P. W. PRICE *et al.*, 2012 Developmental Genetics of Secretory Vesicle Acidification during *Caenorhabditis elegans* Spermatogenesis. Genetics, In Press.

GLEASON, E. J., W. C. LINDSEY, T. L. KROFT, A. W. SINGSON and W. L'HERNAULT S, 2006 *spe-10* encodes a DHHC-CRD zinc-finger membrane protein required for endoplasmic reticulum/Golgi membrane morphogenesis during *Caenorhabditis elegans* spermatogenesis. Genetics **172:** 145-158.

GRAHAM, L. A., K. J. HILL and T. H. STEVENS, 1994 VMA7 encodes a novel 14-kDa subunit of the *Saccharomyces cerevisiae* vacuolar H(+)-ATPase complex. J Biol Chem **269:** 25974-25977.

GRUENBERG, J., 2001 The endocytic pathway: a mosaic of domains. Nat Rev Mol Cell Biol **2:** 721-730.

HANDEL, M. A., 2004 The XY body: a specialized meiotic chromatin domain. Exp Cell Res **296:** 57-63.

HERMAN, R. K., J. E. MADL and C. K. KARI, 1979 Duplications in *Caenorhabditis elegans*. Genetics **92:** 419-435.

HIESINGER, P. R., A. FAYYAZUDDIN, S. Q. MEHTA, T. ROSENMUND, K. L. SCHULZE *et al.*, 2005 The v-ATPase V0 subunit a1 is required for a late step in synaptic vesicle exocytosis in *Drosophila*. Cell **121:** 607-620.

HILL, K. L., 2000 Analyses of Spermatogenesis and the Role of Sperm in Reproductive Interactions in the Nematode Genus *Caenorhabditis*, pp. 276. in *Program in Genetics and Molecular Biology, Graduate Division of Biological and Biomedical Sciences*. Emory University, Atlanta, GA.

HIRATA, R., L. A. GRAHAM, A. TAKATSUKI, T. H. STEVENS and Y. ANRAKU, 1997 VMA11 and VMA16 encode second and third proteolipid subunits of the *Saccharomyces cerevisiae* vacuolar membrane H+-ATPase. J Biol Chem **272:** 4795-4803.

HIRATA, R., Y. OHSUMK, A. NAKANO, H. KAWASAKI, K. SUZUKI *et al.*, 1990 Molecular structure of a gene, VMA1, encoding the catalytic subunit of H(+)-translocating adenosine triphosphatase from vacuolar membranes of *Saccharomyces cerevisiae*. J Biol Chem **265:** 6726-6733.

HO, M. N., R. HIRATA, N. UMEMOTO, Y. OHYA, A. TAKATSUKI *et al.*, 1993 VMA13 encodes a 54-kDa vacuolar H(+)-ATPase subunit required for activity but not assembly of the enzyme complex in *Saccharomyces cerevisiae*. J Biol Chem **268:** 18286-18292.

HODGKIN, J. A., H. R. HORVITZ and S. BRENNER, 1979 Nondisjunction mutants of the nematode *Caenorhabditis elegans*. Genetics **91:** 67-94.

HORVITZ, H. R., S. BRENNER, J. HODGKIN and R. K. HERMAN, 1979 A uniform genetic nomenclature for the nematode *Caenorhabditis elegans*. Mol Gen Genet **175:** 129-133.

HOWELL, A. M., S. G. GILMAR, R. A. MANCEBO and A. M. ROSE, 1987 Genetic analysis of a large autosomal region in *Caenorhabditis elegans* by the use of a free duplication. Genet. Res. **49:** 207-213.

HUYNH, K. K., and S. GRINSTEIN, 2007 Regulation of vacuolar pH and its modulation by some microbial species. Microbiol Mol Biol Rev **71:** 452-462.

KAMATH, R. S., A. G. FRASER, Y. DONG, G. POULIN, R. DURBIN *et al.*, 2003 Systemic functional analysis of the *Caenorhabditis elegans* genome using RNAi. Nature **421:** 231-237.

KANE, P. M., 1995 Disassembly and reassembly of the yeast vacuolar H(+)-ATPase *in vivo*. J Biol Chem **270:** 17025-17032.

KANE, P. M., 2006 The where, when, and how of organelle acidification by the yeast vacuolar H+-ATPase. Microbiol Mol Biol Rev **70:** 177-191.

KAWASAKI-NISHI, S., K. BOWERS, T. NISHI, M. FORGAC and T. H. STEVENS, 2001a The amino-terminal domain of the vacuolar proton-translocating ATPase a subunit controls targeting and *in vivo* dissociation, and the carboxyl-terminal domain affects coupling of proton transport and ATP hydrolysis. J Biol Chem **276:** 47411-47420.

KAWASAKI-NISHI, S., T. NISHI and M. FORGAC, 2001b Yeast V-ATPase complexes containing different isoforms of the 100-kDa a-subunit differ in coupling efficiency and *in vivo* dissociation. J Biol Chem **276:** 17941-17948.

KELLY, W. G., and A. FIRE, 1998 Chromatin silencing and the maintenance of a functional germline in *Caenorhabditis elegans*. Development **125:** 2451-2456.

KELLY, W. G., C. E. SCHANER, A. F. DERNBURG, M. H. LEE, S. K. KIM *et al.*, 2002 X-chromosome silencing in the germline of *C. elegans*. Development **129:** 479-492.

KETEL, C. S., E. F. ANDERSEN, M. L. VARGAS, J. SUH, S. STROME *et al.*, 2005 Subunit contributions to histone methyltransferase activities of fly and worm polycomb group complexes. Mol Cell Biol **25:** 6857-6868.

KLASS, M. R., and D. HIRSH, 1981 Sperm isolation and biochemical analysis of the major sperm protein from *Caenorhabditis elegans*. Developmental Biology **84:** 299-312.

L'HERNAULT, S. W., 2006 Spermatogenesis. *WormBook*: doi/10. 1895/wormbook. 1.85.1.

L'HERNAULT, S. W., and P. M. ARDUENGO, 1992 Mutation of a putative sperm membrane protein in *Caenorhabditis elegans* prevents sperm differentiation but not its associated meiotic divisions. J Cell Biol **119:** 55-68.

L'HERNAULT, S. W., G. M. BENIAN and R. B. EMMONS, 1993 Genetic and molecular characterization of the *Caenorhabditis elegans* spermatogenesis-defective gene *spe-17*. Genetics **134:** 769-780.

LIEGEOIS, S., A. BENEDETTO, J. M. GARNIER, Y. SCHWAB and M. LABOUESSE, 2006 The V0-ATPase mediates apical secretion of exosomes containing Hedgehog-related proteins in *Caenorhabditis elegans*. J Cell Biol **173:** 949-961.

LU, M., Y. Y. SAUTIN, L. S. HOLLIDAY and S. L. GLUCK, 2004 The glycolytic enzyme aldolase mediates assembly, expression, and activity of vacuolar H+-ATPase. J Biol Chem **279:** 8732-8739.

MACHACA, K., and S. W. L'HERNAULT, 1997 The *Caenorhabditis elegans spe-5* gene is required for morphogenesis of a sperm-specific organelle and is associated with an inherent cold-sensitive phenotype. Genetics **146:** 567-581.

MACIEJOWSKI, J., J. H. AHN, P. G. CIPRIANI, D. J. KILLIAN, A. L. CHAUDHARY *et al.*, 2005 Autosomal genes of autosomal/X-linked duplicated gene pairs and germ-line proliferation in *Caenorhabditis elegans*. Genetics **169:** 1997-2011.

MANOLSON, M. F., B. WU, D. PROTEAU, B. E. TAILLON, B. T. ROBERTS *et al.*, 1994 STV1 gene encodes functional homologue of 95-kDa yeast vacuolar H(+)-ATPase subunit Vph1p. J Biol Chem **269:** 14064-14074.

MUHLRAD, P. J., and S. WARD, 2002 Spermiogenesis initiation in *Caenorhabditis elegans* involves a casein kinase 1 encoded by the *spe-6* gene. Genetics **161:** 143-155.

MULLER, M. L., U. IRKENS-KIESECKER, D. KRAMER and L. TAIZ, 1997 Purification and reconstitution of the vacuolar H+-ATPases from lemon fruits and epicotyls. J Biol Chem **272:** 12762-12770.

MURATA, T., I. YAMATO, Y. KAKINUMA, A. G. LESLIE and J. E. WALKER, 2005 Structure of the rotor of the V-Type Na+-ATPase from *Enterococcus hirae*. Science **308:** 654-659.

NELSON, G. A., T. M. ROBERTS and S. WARD, 1982 *Caenorhabditis elegans* spermatozoan locomotion: amoeboid movement with almost no actin. J Cell Biol **92:** 121-131.

NELSON, H., S. MANDIYAN and N. NELSON, 1995 A bovine cDNA and a yeast gene (VMA8) encoding the subunit D of the vacuolar H(+)-ATPase. Proc Natl Acad Sci U S A **92:** 497-501.

NISHI, T., and M. FORGAC, 2002 The vacuolar (H+)-ATPases--nature's most versatile proton pumps. Nat Rev Mol Cell Biol **3:** 94-103.

NISHIMURA, H., and S. W. L'HERNAULT, 2010 Spermatogenesis-defective (*spe*) mutants of the nematode *Caenorhabditis elegans* provide clues to solve the puzzle of male germline functions during reproduction. Dev Dyn **239:** 1502-1514.

OKA, T., T. TOYOMURA, K. HONJO, Y. WADA and M. FUTAI, 2001 Four subunit a isoforms of *Caenorhabditis elegans* vacuolar H+-ATPase. Cell-specific expression during development. J Biol Chem **276:** 33079-33085.

OWEGI, M. A., D. L. PAPPAS, M. W. FINCH, JR., S. A. BILBO, C. A. RESENDIZ *et al.*, 2006 Identification of a domain in the V0 subunit d that is critical for coupling of the yeast vacuolar proton-translocating ATPase. J Biol Chem **281:** 30001-30014.

PUJOL, N., C. BONNEROT, J. J. EWBANK, Y. KOHARA and D. THIERRY-MIEG, 2001 The *Caenorhabditis elegans unc-32* gene encodes alternative forms of a vacuolar ATPase a subunit. J Biol Chem **276:** 11913-11921.

REINKE, V., I. S. GIL, S. WARD and K. KAZMER, 2004 Genome-wide germline-enriched and sex-biased expression profiles in *Caenorhabditis elegans*. Development **131:** 311-323.

REINKE, V., H. E. SMITH, J. NANCE, J. WANG, C. VAN DOREN *et al.*, 2000 A global profile of germline gene expression in *C. elegans*. Mol Cell **6:** 605-616.

RIDDLE, D. L., and P. S. ALBERT, 1997 Genetic and environmental regulation of dauer larva development, pp. 739-768 in *C. elegans II*, edited by D. RIDDLE, R. BLUMENTHAL, B. J. MEYER and J. PRIESS. Cold Spring Harbor Press, Cold Spring Harbor, NY.

ROBERTS, T. M., F. M. PAVALKO and S. WARD, 1986 Membrane and cytoplasmic proteins are transported in the same organelle complex during nematode spermatogenesis. J Cell Biol **102:** 1787-1796.

ROBERTS, T. M., and S. WARD, 1982 Centripetal flow of pseudopodial surface components could propel the amoeboid movement of *Caenorhabditis elegans* spermatozoa. J Cell Biol **92:** 132-138.

SCIMECA, J. C., A. FRANCHI, C. TROJANI, H. PARRINELLO, J. GROSGEORGE *et al.*, 2000 The gene encoding the mouse homologue of the human osteoclast-specific 116-kDa V-ATPase subunit bears a deletion in osteosclerotic (oc/oc) mutants. Bone **26:** 207-213.

SHAKES, D. C., and S. WARD, 1989 Mutations that disrupt the morphogenesis and localization of a sperm-specific organelle in *Caenorhabditis elegans*. Dev Biol **134:** 307-316.

SHAO, E., T. NISHI, S. KAWASAKI-NISHI and M. FORGAC, 2003 Mutational analysis of the non-homologous region of subunit A of the yeast V-ATPase. J Biol Chem **278:** 12985-12991.

STEVENS, T. H., and M. FORGAC, 1997 Structure, function and regulation of the vacuolar (H+)-ATPase. Annu Rev Cell Dev Biol **13:** 779-808.

SUN-WADA, G. H., H. TABATA, N. KAWAMURA, M. FUTAI and Y. WADA, 2007 Differential expression of a subunit isoforms of the vacuolar-type proton pump ATPase in mouse endocrine tissues. Cell Tissue Res **329:** 239-248.

SUPEKOVA, L., F. SUPEK and N. NELSON, 1995 The *Saccharomyces cerevisiae* VMA10 is an intron-containing gene encoding a novel 13-kDa subunit of vacuolar H(+)-ATPase. J Biol Chem **270:** 13726-13732.

UMEMOTO, N., Y. OHYA and Y. ANRAKU, 1991 VMA11, a novel gene that encodes a putative proteolipid, is indispensable for expression of yeast vacuolar membrane H(+)-ATPase activity. J Biol Chem **266:** 24526-24532.

VARKEY, J. P., P. L. JANSMA, A. N. MINNITI and S. WARD, 1993 The *Caenorhabditis elegans spe-6* gene is required for major sperm protein assembly and shows second site non-complementation with an unlinked deficiency. Genetics **133:** 79-86.

WARD, S., Y. ARGON and G. A. NELSON, 1981 Sperm morphogenesis in wild-type and fertilization-defective mutants of *Caenorhabditis elegans*. J Cell Biol **91:** 26-44.

WARD, S., and J. S. CARREL, 1979 Fertilization and sperm competition in the nematode *Caenorhabditis elegans*. Dev Biol **73:** 304-321.

WARD, S., E. HOGAN and G. A. NELSON, 1983 The initiation of spermiogenesis in the nematode *Caenorhabditis elegans*. Dev Biol **98:** 70-79.

WARD, S., and M. KLASS, 1982 The location of the major protein in *Caenorhabditis elegans* sperm and spermatocytes. Dev Biol **92:** 203-208.

WARD, S., T. M. ROBERTS, S. STROME, F. M. PAVALKO and E. HOGAN, 1986 Monoclonal antibodies that recognize a polypeptide antigenic determinant shared by multiple *Caenorhabditis elegans* sperm-specific proteins. J Cell Biol **102:** 1778-1786.

WOLF, N., D. HIRSH and J. R. MCINTOSH, 1978 Spermatogenesis in males of the free-living nematode, *Caenorhabditis elegans*. J Ultrastruct Res **63:** 155-169.

XIA, W., and M. S. WOLFE, 2003 Intramembrane proteolysis by presenilin and presenilin-like proteases. J Cell Sci **116:** 2839-2844.

XU, L., Y. FONG and S. STROME, 2001 The *Caenorhabditis elegans* maternal-effect sterile proteins, MES-2, MES- 3, and MES-6, are associated in a complex in embryos. Proc Natl Acad Sci U S A **98:** 5061-5066.

ZHU, G. D., and S. W. L'HERNAULT, 2003 The *Caenorhabditis elegans spe-39* gene is required for intracellular membrane reorganization during spermatogenesis. Genetics **165:** 145-157.

ZHU, G. D., G. SALAZAR, S. A. ZLATIC, B. FIZA, M. M. DOUCETTE *et al.*, 2009 SPE-39 family proteins interact with the HOPS complex and function in lysosomal delivery. Mol Biol Cell **20:** 1223-1240.

Tables and Figures

Figure 1- **A.** An overview of spermatogenesis. **B.** A summary of morphogenesis of the FB-MO complex. (L'HERNAULT 2006)

Figure 2- An overview of representative genes known to be associated with spermatogenesis or fertilization. (L'HERNAULT 2006).

Figure 3- The structure of the V-ATPase complex is shown. The two sectors V_O and V_1 are shown. V_O is embedded in the lipid bilayer of a membrane. Taken from Wikipedia V-ATPase article.

Figure 4- pRW05(top) and pVK7(bottom) Introduction of *Xma* I sites 5' and 3' would not affect the reading frame for *spe-5* during protein synthesis as *Xma* I is a six cutter and thus would alter the open reading frame of SPE-5. RNA transcription would transcribe the 2 codons from the recognition site but protein synthesis would start at the start codon.

Figure 5- Experimental schematic showing insertion of a *Xma* I recognition site in place of the *vha-12* coding sequence in pRW05. **A.** First round PCR to insert a *Xma* I recognition site in place of *vha-12* coding sequence. Two fragments result with one fragment containing a *Xma* I site and a 5' flanking sequence and another with a *Xma* I and a 3' flanking sequence. The portion of the *Xma* I primers that contain the recognition sequence do not initially bind to another single stranded DNA strand but after 1 cycle the *Xma* I will bind to the reverse complement. Two products are formed in the first round of PCR and will be used in the second round of PCR**.** Note that the template DNA for this reaction (pRW05) is a plasmid

and is shown as a linear segment for better visualization. **B.** Second round PCR to have the *Xma* I site with flanking regions both 5' and 3' so that it can be ligated into pRW04, thus resulting in a *Xma* I site in place of *vha-12.* **C.** Restriction digests of both the second round PCR product and pRW05 and subsequent ligation to yield pVK1 (pRW05 with 1 *Xma* I site).

Figure 6- PCR reaction to insert *Xma* I sites 5' and 3' of *spe-5.* Initially this PCR produced incorrect products due to non-specific binding of primers. Longer primers with higher Tm's were then used (See Table 1). BS-0636 is a plasmid and is shown as linear segment for better visualization.

Figure 7- Diagram outlining the restriction digests of PCR2.1 with the *spe-5* PCR product and pVK2 with *Xma* I. The resulting bands (1.6 kb for *spe-5* and 7.8 kb from pVK2) from gel electrophoresis were cut, purified and subsequently ligated to yield pVK7.

Figure 8- Outline of how a construct containing two *spe-5* inserts was altered to yield a plasmid with only one *spe-5* coding sequence.

Figure 9- Summary of *ebEX*/*spe-5 dpy* x *met-2* cross. *ebEX*/*spe-5 dpy-5* had to be first crossed into *unc-32* so that *met-2*(which has no visible phenotype) could be followed.

Figure 10- Graph showing increased brood size of *spe-5* mutants *and spe-5 him-5* double mutants with RNAi knockdown of *mes-4*.

Figure 11- Brood sizes comparing *spe-5* mutants *and spe-5 him-5* double mutants with RNAi knockdown of *mes-4*.

Figure 12- Graph showing no significant changes in brood size when *spe-5* mutants are crossed into *met-2* mutants.

Figure 13- **A.** DIC fluorescence microscopy of wild type spermatids. **B.** The position and staining of wild type MO secretory vesicles with Lysosensor Blue DND-192 during C. *elegans* spermatogenesis. Arrows point to acidified vesicles. **C.** Wild-type spermatids treated with 70mM TEA pH 7.8. **D.** Arrested spermatocytes in *spe-5(ok1054)* mutants that were fed bacteria containing the L4440 blank vector as a RNAi control.

Figure 14- **A, D**- DIC image of *spe-5* mutant spermatids with knockdown of *mes-4* via RNAi. **B,E –**Lysosensor Blue DND-192 staining of *spe-5* mutant spermatids with knockdown of *mes-4* via RNAi. **F.** DIC image of *spe-5* mutant spermatids with knockdown of *met-2* via RNAi. **G.** Lysosensor Blue DND-192 staining of *spe-5* mutant spermatids with knockdown of *met-2* via RNAi. **H.** DIC image of *hc93 spe-5* mutant spermatids (taken by Elizabeth Gleason). **I.** Lysosensor Blue DND-192 staining of *hc93 spe-5* mutant spermatids (taken by Elizabeth Gleason).

Table 1- Sequences of Primers used in PCR experiments.

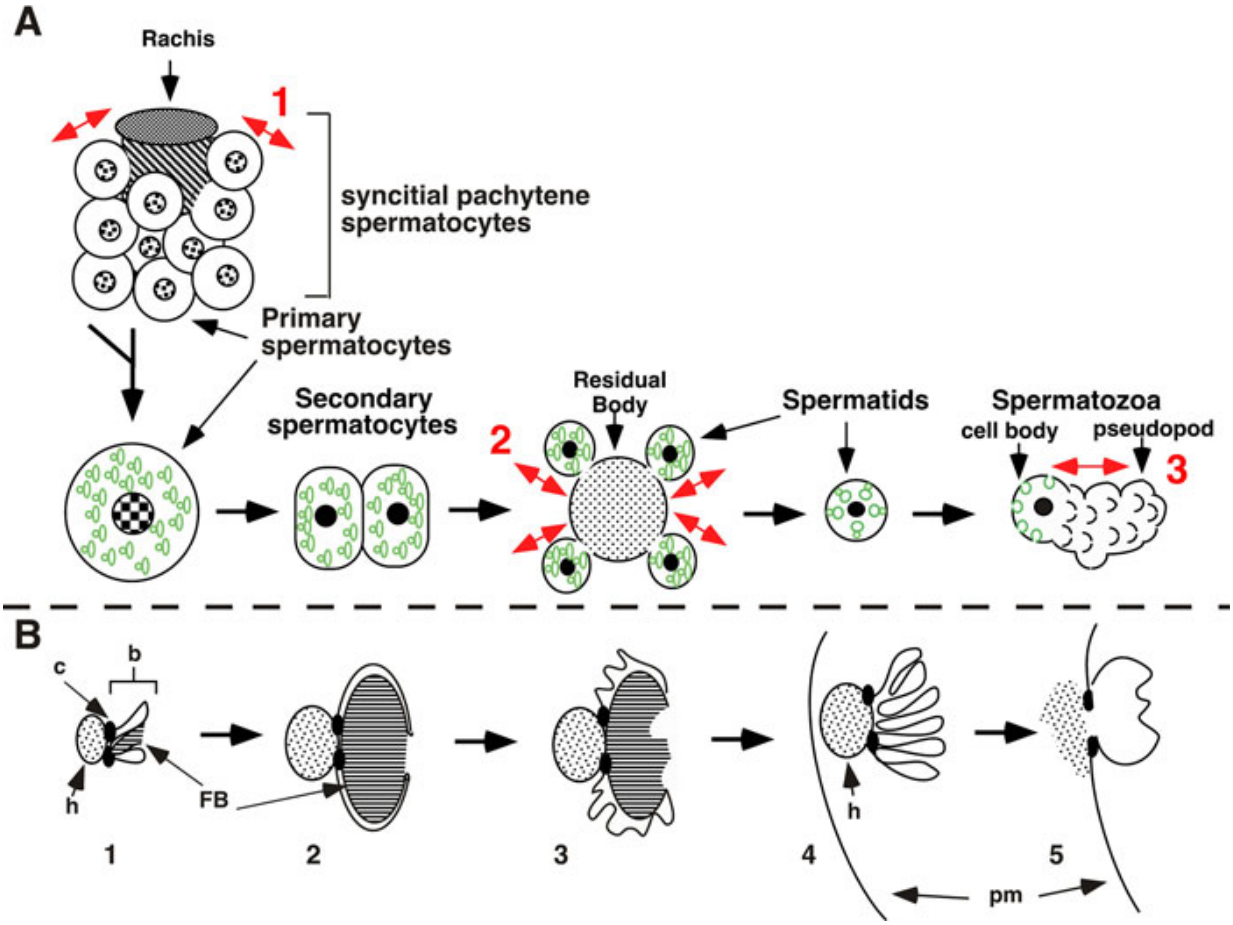
A
Rachis
1
syncitial pachytene spermatocytes
Primary spermatocytes
Secondary spermatocytes
Residual Body
2
Spermatids
Spermatozoa
cell body
pseudopod
3
B
c
b
h
FB
1
2
3
4
h
5
pm

Figure 1

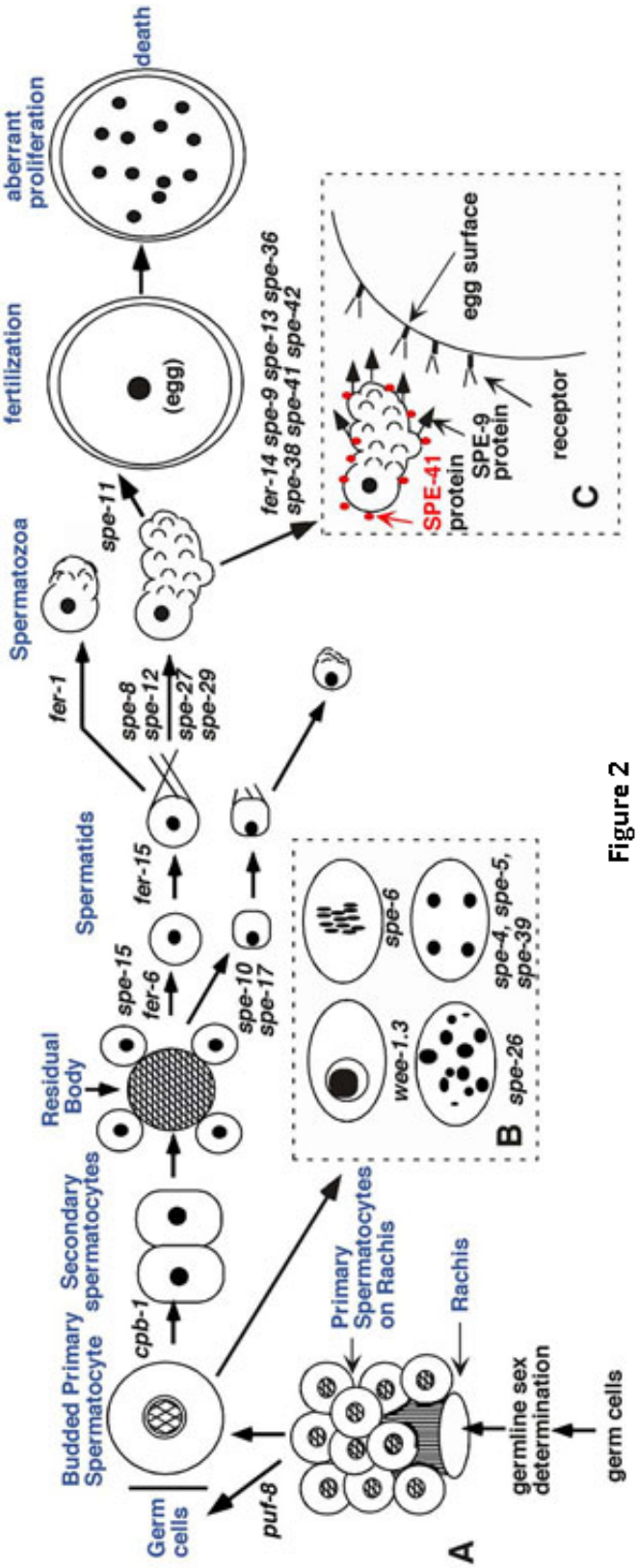
germ cells
germline sex determination
Rachis
Primary Spermatocytes on Rachis
Budded Primary Spermatocyte
Secondary spermatocytes
Residual Body
Spermatids
Spermatozoa
fertilization
aberrant proliferation
death
(egg)
egg surface
receptor
SPE-9 protein
SPE-41 protein
A
B
C
puf-8
cpb-1
spe-15
fer-6
fer-15
spe-10
spe-17
fer-1
spe-8
spe-12
spe-27
spe-29
spe-11
fer-14 spe-9 spe-13 spe-36
spe-38 spe-41 spe-42
wee-1.3
spe-26
spe-6
spe-4, spe-5,
spe-39

Figure 2

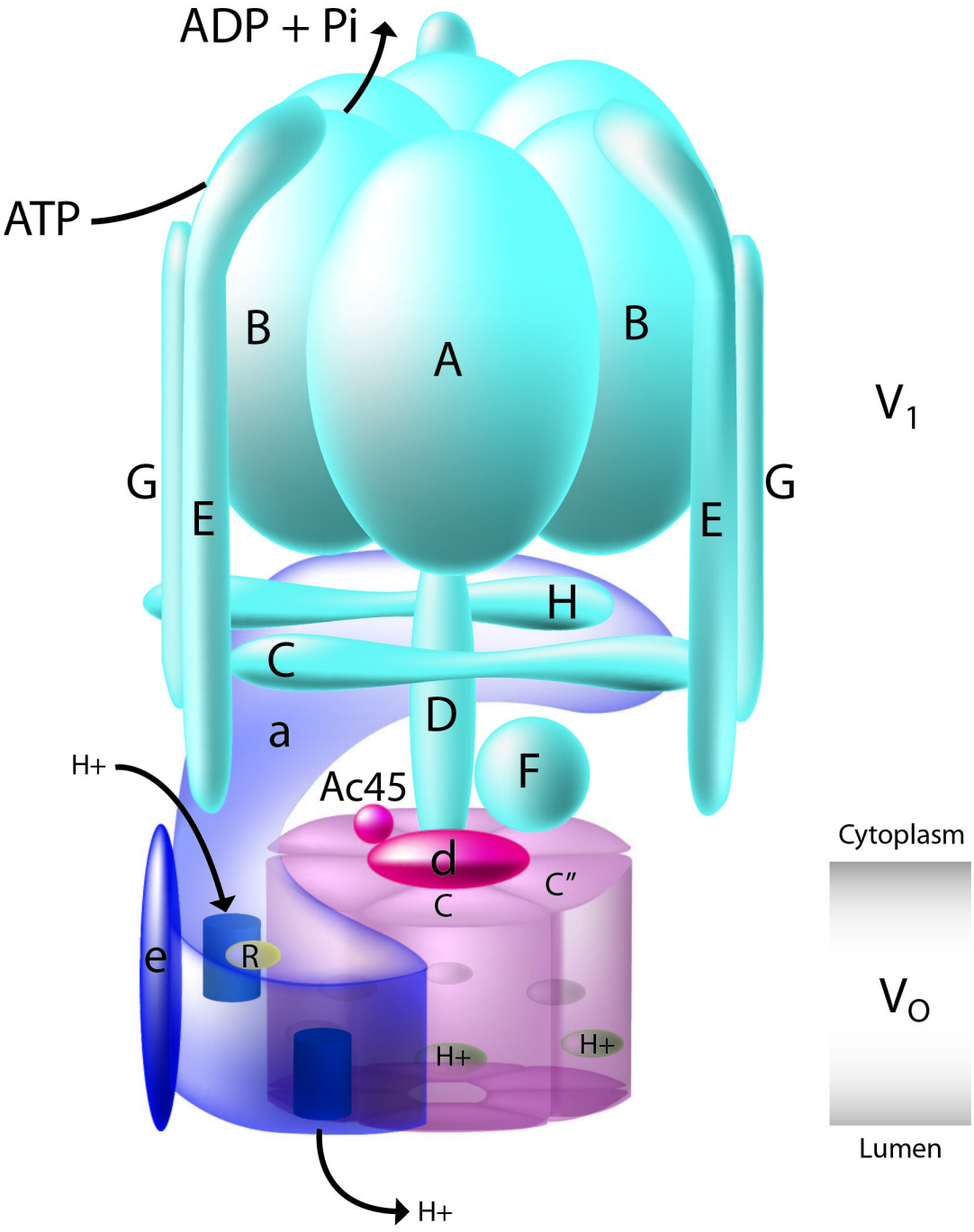
ADP + Pi
ATP
B
A
B
V1
G
E
E
G
H
C
D
a
H+
Ac45
F
d
C
C″
e
R
H+
H+
H+
Cytoplasm
VO
Lumen

Figure 3

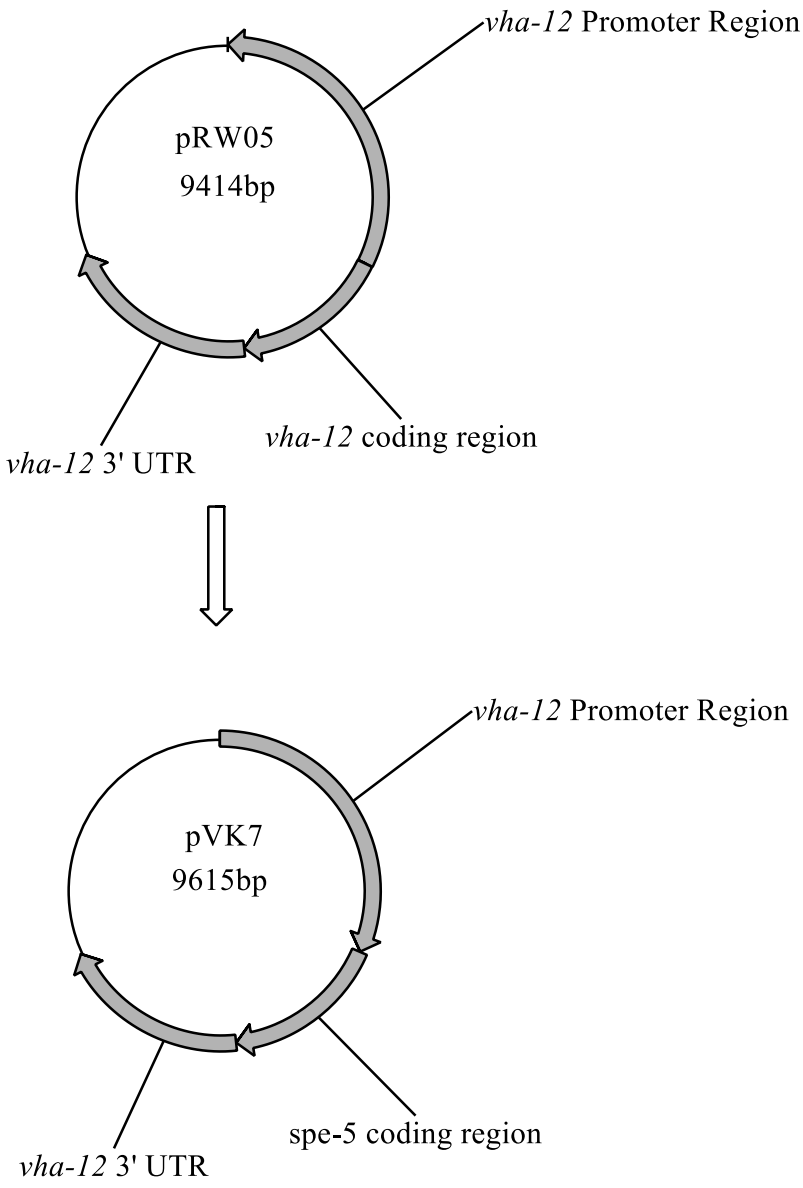
vha-12 Promoter Region
pRW05
9414bp
vha-12 coding region
vha-12 3' UTR
vha-12 Promoter Region
pVK7
9615bp
spe-5 coding region
vha-12 3' UTR

Figure 4

A.

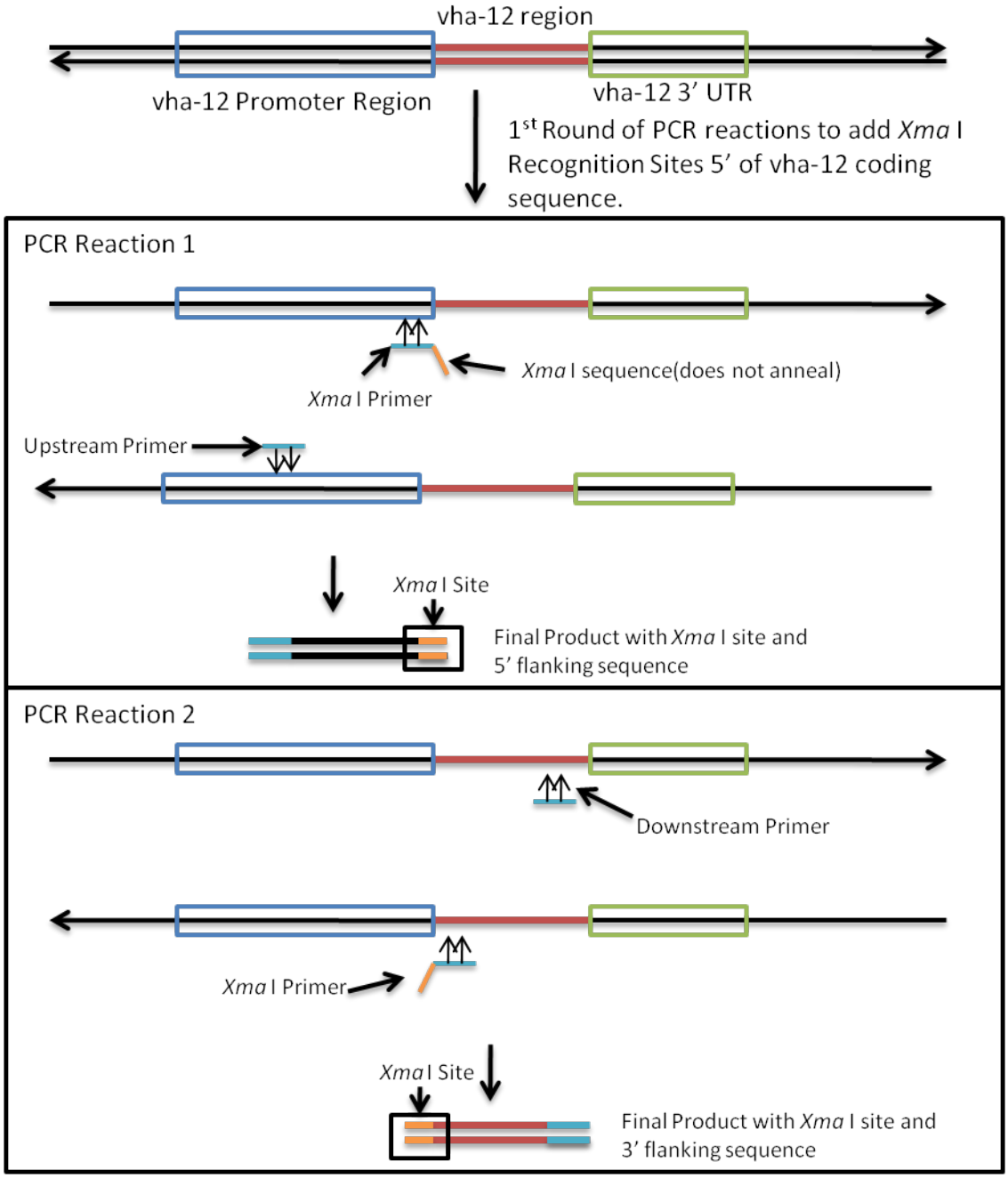
vha-12 region
vha-12 Promoter Region
vha-12 3' UTR
1st Round of PCR reactions to add Xma I Recognition Sites 5' of vha-12 coding sequence.
PCR Reaction 1
Xma I sequence(does not anneal)
Xma I Primer
Upstream Primer
Xma I Site
Final Product with Xma I site and 5' flanking sequence
PCR Reaction 2
Downstream Primer
Xma I Primer
Xma I Site
Final Product with Xma I site and 3' flanking sequence

Figure 5(A)

B.

2nd Round PCR to synthesize segment that contains the 5' *Xma* I recognition for insertion into pRW05 via Restriction Digest

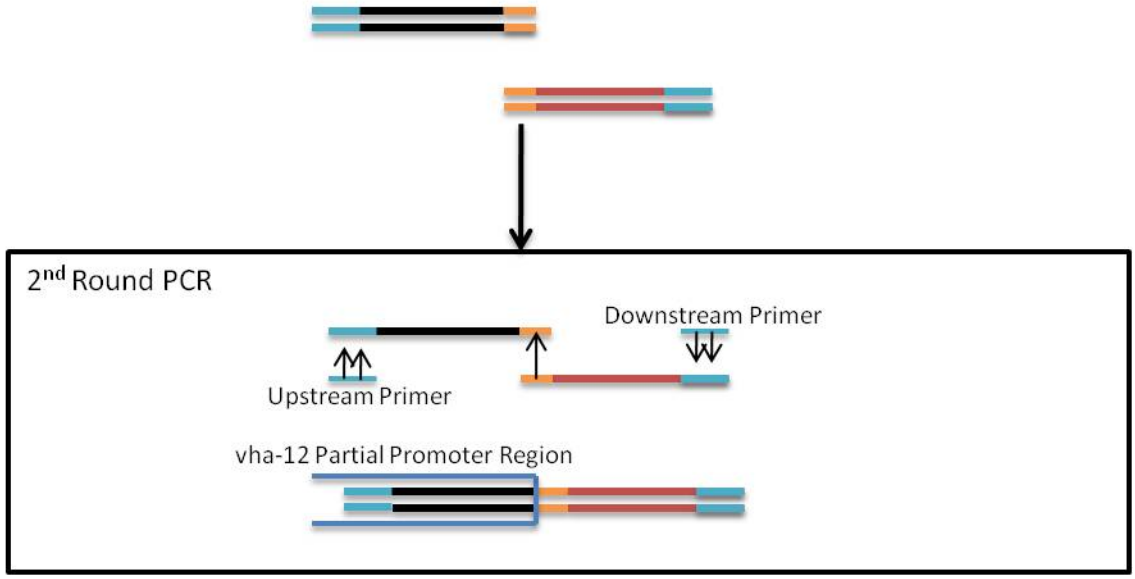

C.

Insertion of 5' *Xma* I recognition site into pRW05 via Restriction Digest

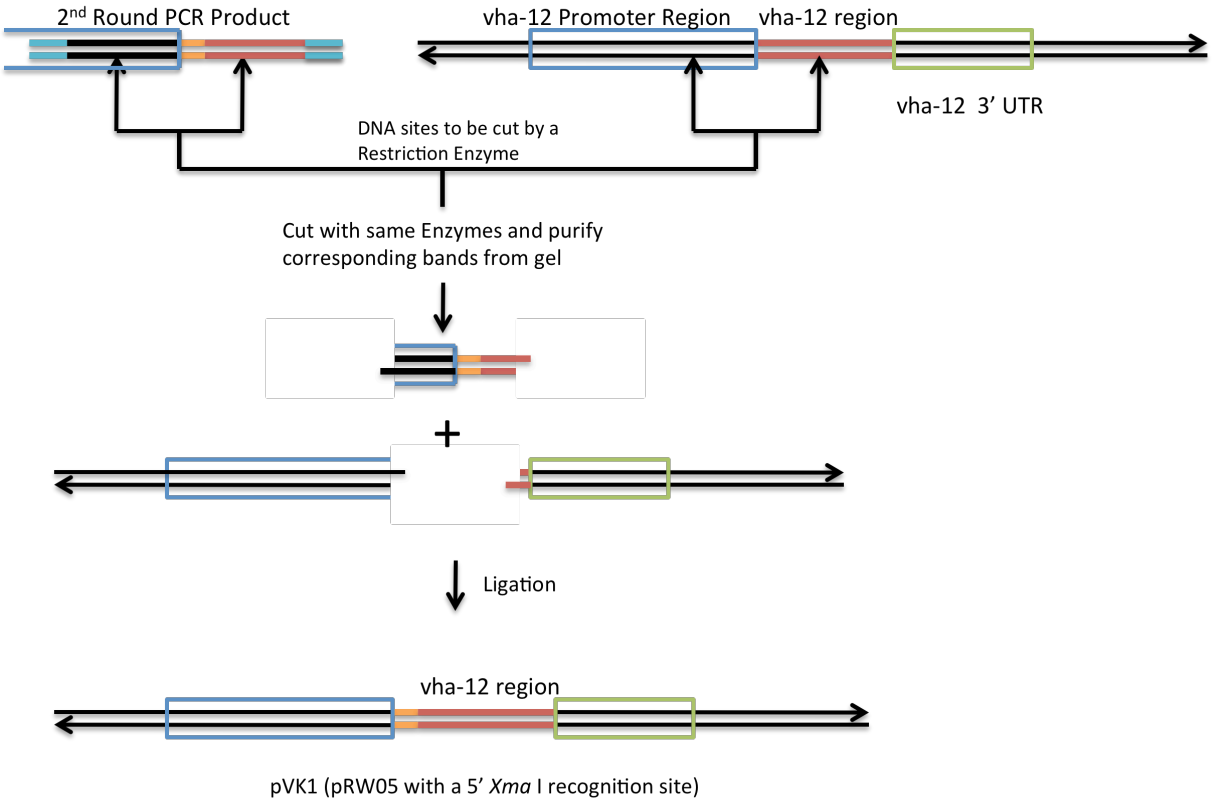

pVK1 (pRW05 with a 5' *Xma* I recognition site)

Figure 5(B-C)

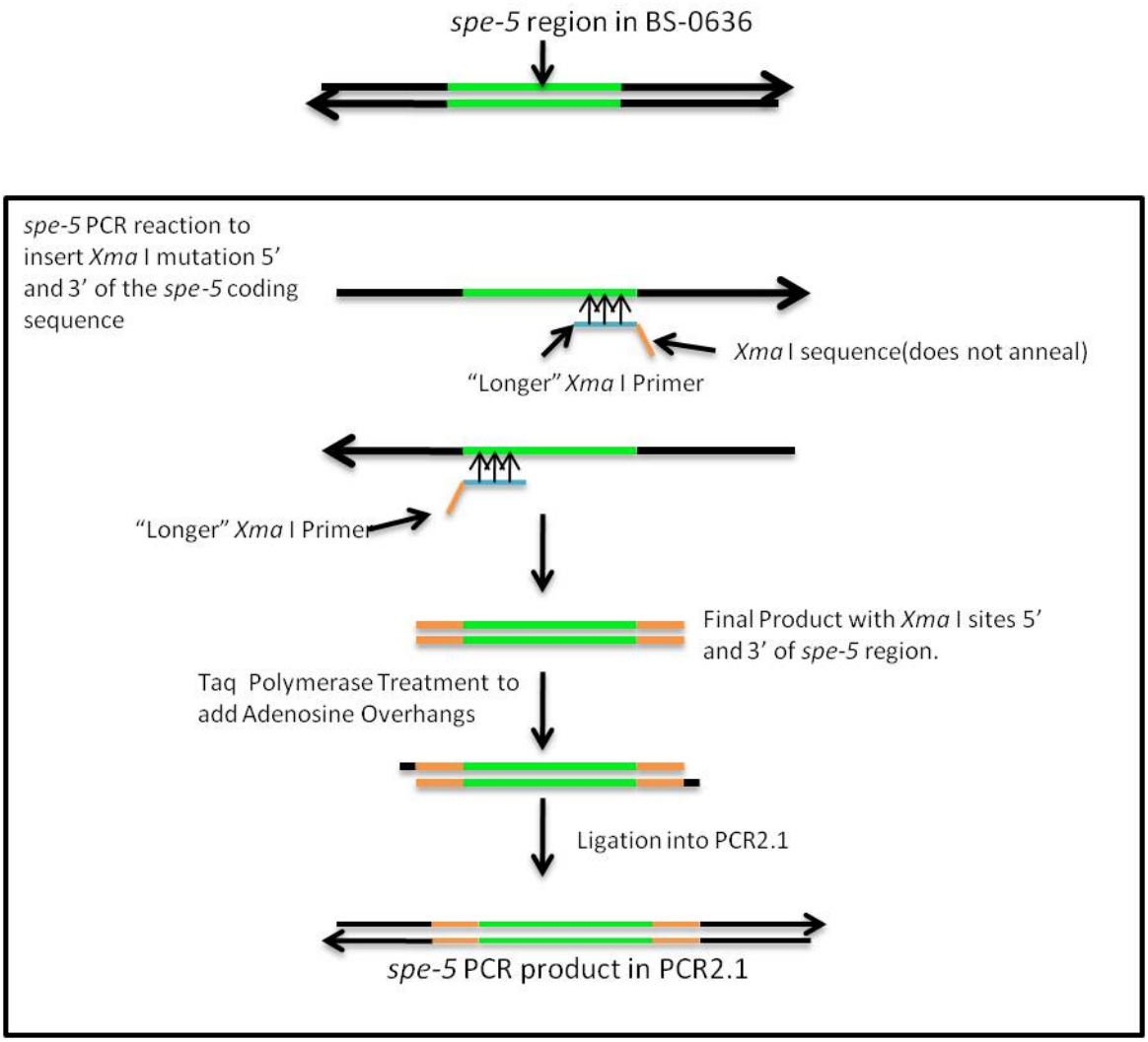
spe-5 region in BS-0636
spe-5 PCR reaction to insert *Xma* I mutation 5' and 3' of the *spe-5* coding sequence
Xma I sequence(does not anneal)
"Longer" *Xma* I Primer
"Longer" *Xma* I Primer
Final Product with *Xma* I sites 5' and 3' of *spe-5* region.
Taq Polymerase Treatment to add Adenosine Overhangs
Ligation into PCR2.1
spe-5 PCR product in PCR2.1

Figure 6

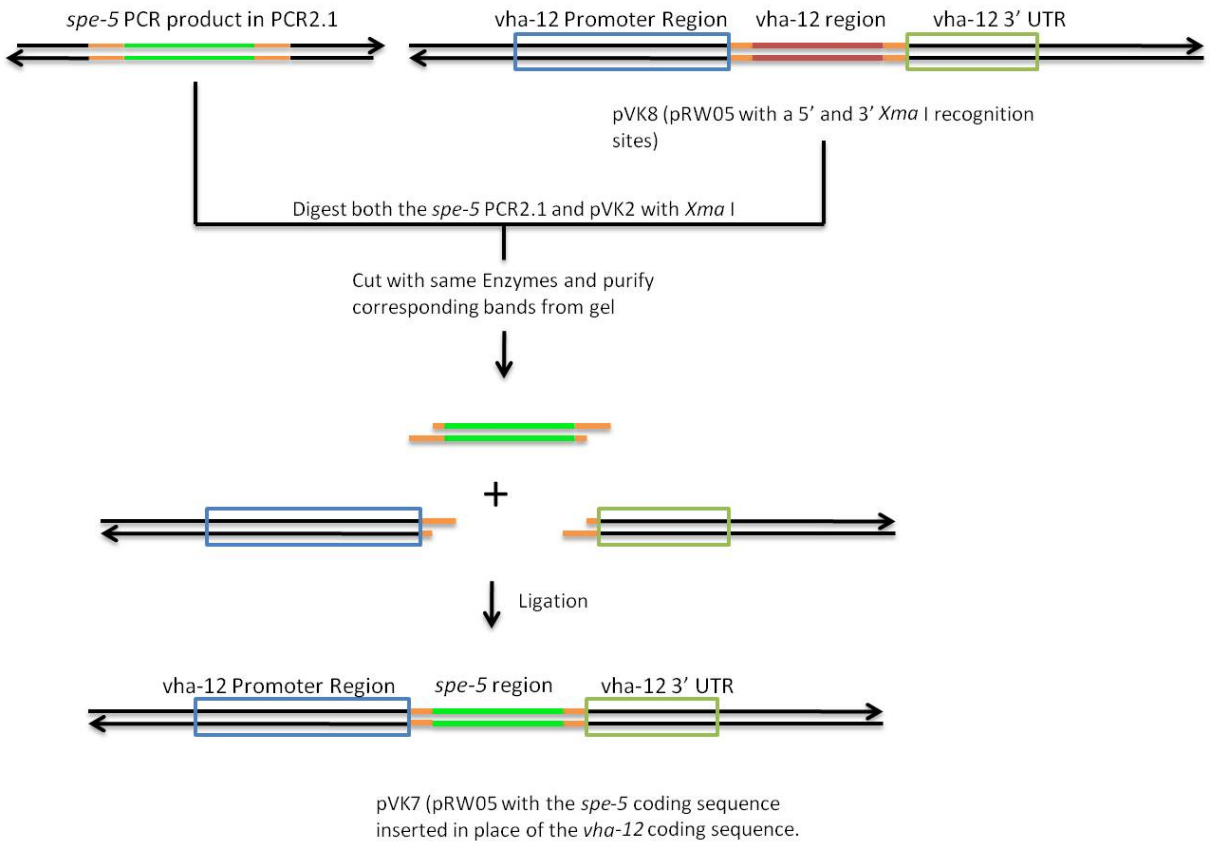
spe-5 PCR product in PCR2.1
vha-12 Promoter Region
vha-12 region
vha-12 3' UTR
pVK8 (pRW05 with a 5' and 3' Xma I recognition sites)
Digest both the spe-5 PCR2.1 and pVK2 with Xma I
Cut with same Enzymes and purify corresponding bands from gel
+
Ligation
vha-12 Promoter Region
spe-5 region
vha-12 3' UTR
pVK7 (pRW05 with the spe-5 coding sequence inserted in place of the vha-12 coding sequence.

Figure 7

A.

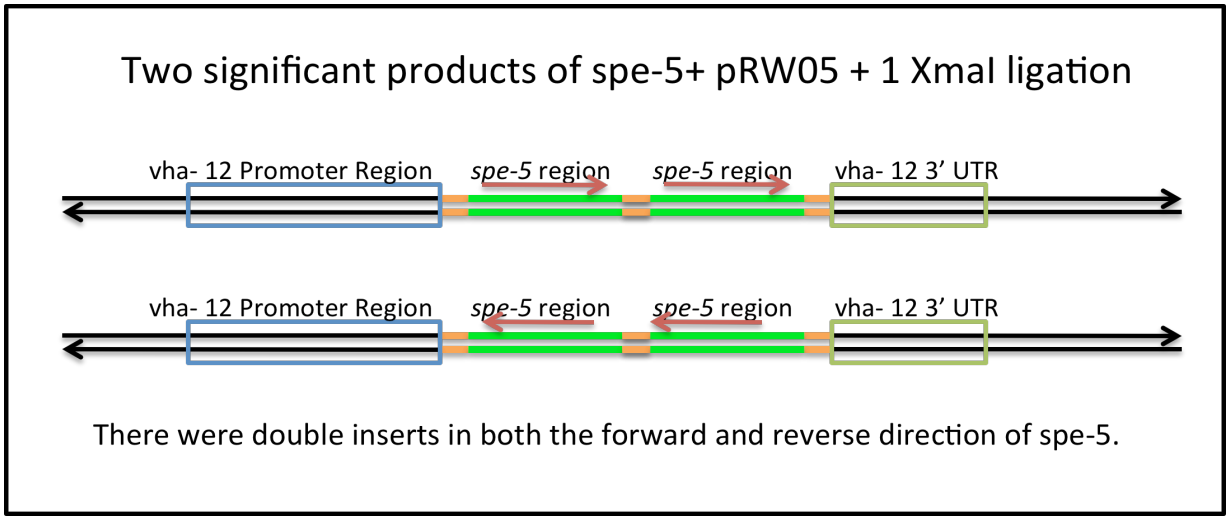
Two significant products of spe-5+ pRW05 + 1 XmaI ligation
vha- 12 Promoter Region
spe-5 region
spe-5 region
vha- 12 3' UTR
vha- 12 Promoter Region
spe-5 region
spe-5 region
vha- 12 3' UTR
There were double inserts in both the forward and reverse direction of spe-5.

Figure 8 (A)

B.

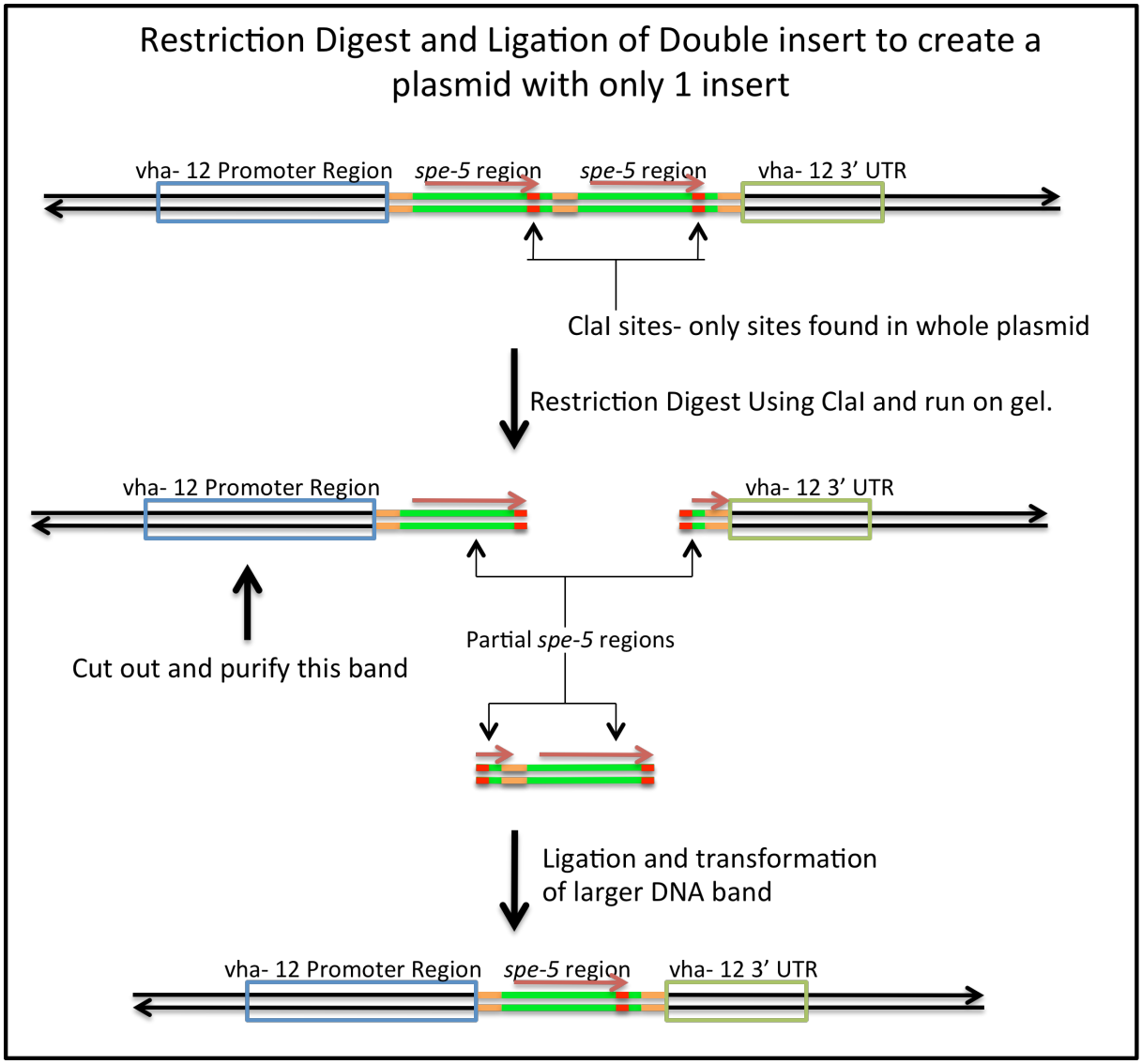
Restriction Digest and Ligation of Double insert to create a plasmid with only 1 insert
vha- 12 Promoter Region
spe-5 region
spe-5 region
vha- 12 3' UTR
ClaI sites- only sites found in whole plasmid
Restriction Digest Using ClaI and run on gel.
vha- 12 Promoter Region
vha- 12 3' UTR
Cut out and purify this band
Partial spe-5 regions
Ligation and transformation of larger DNA band
vha- 12 Promoter Region
spe-5 region
vha- 12 3' UTR

Figure 8 (B)

ebEX/ *spe-5* dpy-5 x *unc-32*

♂ ebEX/*spe-5* dpy-5/*spe-5* dpy-5(I); him-5(V) x ⚥ *unc-32*/ *unc-32* (III)

F1- Non- unc and gfp+

⚥ ebEX/*spe-5* dpy-5/++(I); *unc-32*/+ (III); him-5/+

self and look for gfp+ dpy's that are unc

ebEX/*spe-5* dpy-5/ *spe-5* dpy-5 (I); *unc-32*/ *unc-32* (III)

ebEX x *met-2*

♂ *met-2*/ *met-2*(III) x ⚥ ebEX/*spe-5* dpy-5/*spe-5* dpy-5(I); *unc-32*/ *unc-32* (III)

F1- Non- unc and gfp+

⚥ ebEX/*spe-5* dpy-5/++(I); *unc-32*/*met-2*(III)

Allow heterozygous hermaphrodites to self and look for non-unc dpy's

ebEX/*spe-5* dpy-5/ *spe-5* dpy-5 (I); *met-2*/*met-2*(III)

Follow for at least another generation to ensure loss of *unc-32*

Figure 9

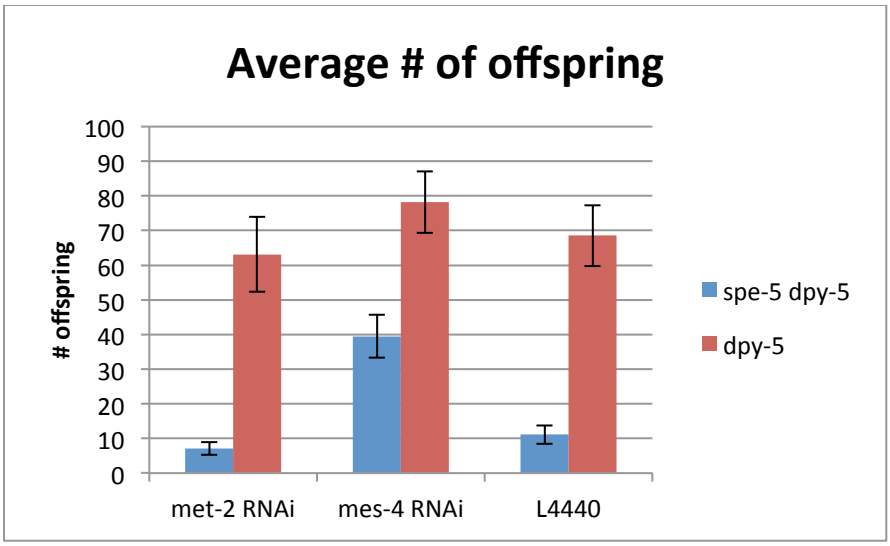

Average # of offspring	*met-2* RNAi	*mes-4* RNAi	L4440
spe-5 dpy-5	7.12	39.46	11.15
dpy-5	63.15	78.20	68.53
Standard Error			
spe-5 dpy-5	1.82	6.22	2.69
dpy-5	10.87	8.93	8.78

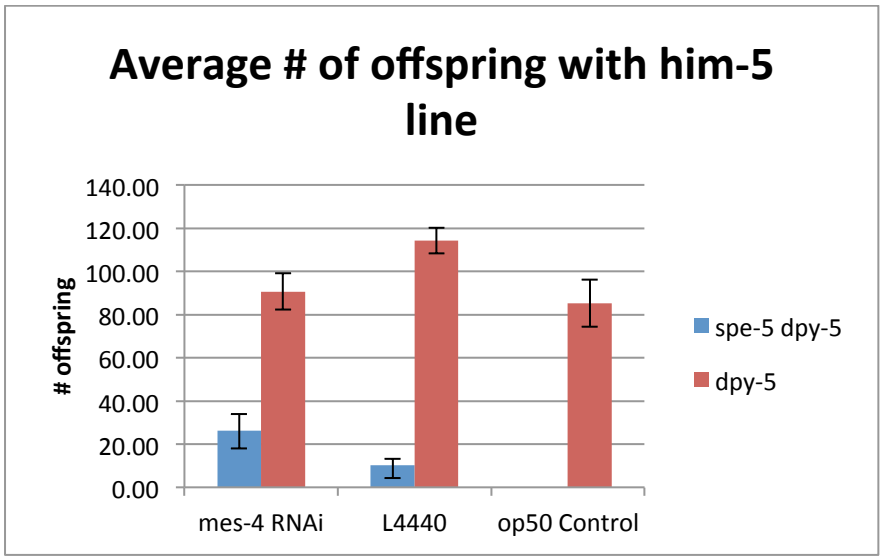

Average # of Offspring	*mes-4* RNAi	L4440	op50 Control
spe-5 dpy-5; him-5	26.35	10.21	
dpy-5; him-5	90.64	114.23	85.31
Standard Error			
spe-5 dpy-5; him-5	7.52	2.98	
dpy-5; him-5	8.34	5.92	10.95

Figure 10

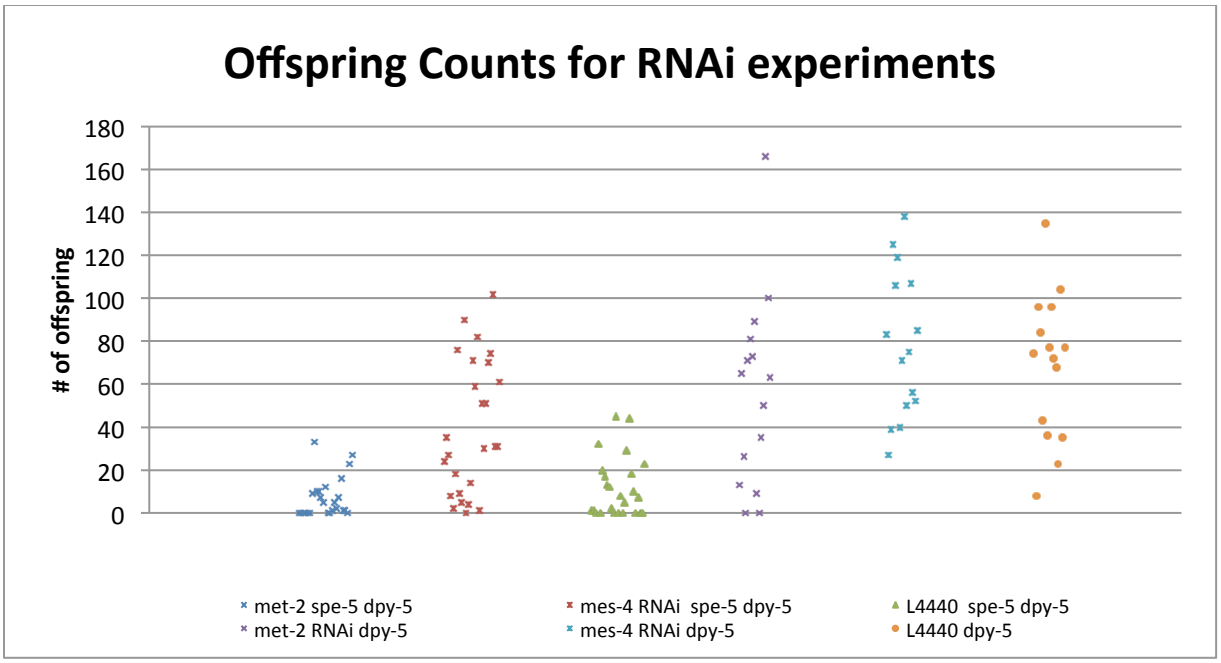
Offspring Counts for RNAi experiments
# of offspring
180
160
140
120
100
80
60
40
20
0
met-2 spe-5 dpy-5
mes-4 RNAi spe-5 dpy-5
L4440 spe-5 dpy-5
met-2 RNAi dpy-5
mes-4 RNAi dpy-5
L4440 dpy-5

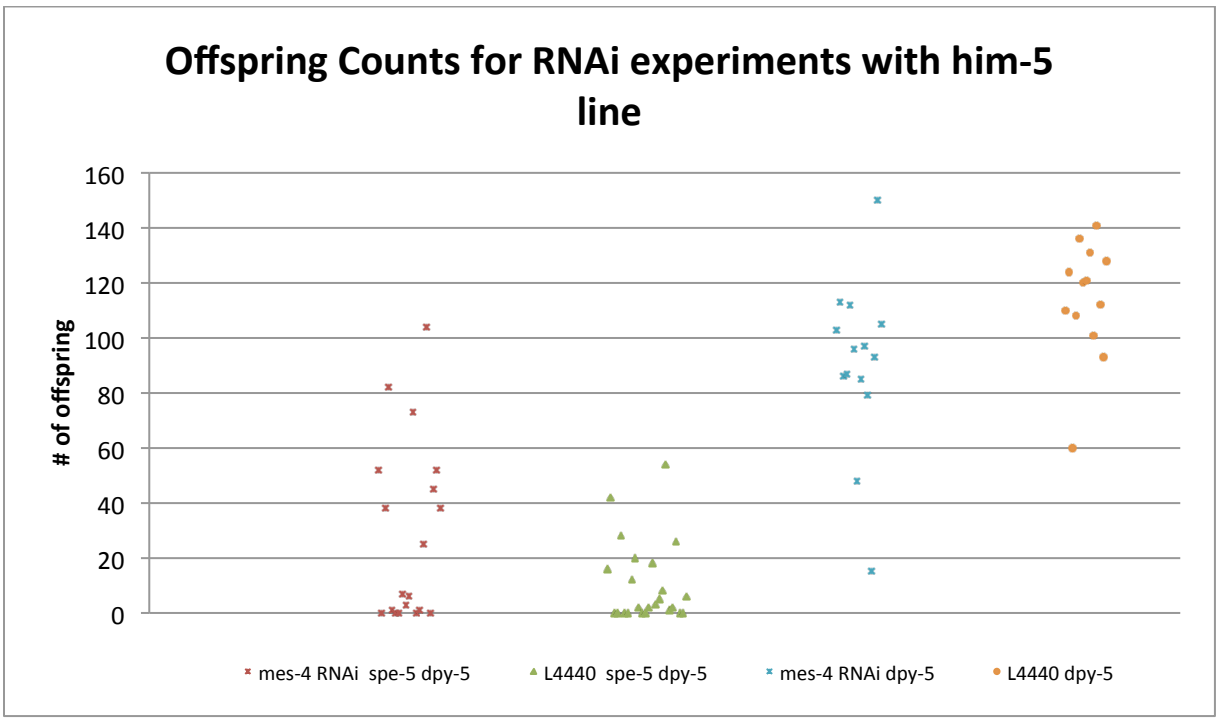
Offspring Counts for RNAi experiments with him-5 line
# of offspring
160
140
120
100
80
60
40
20
0
mes-4 RNAi spe-5 dpy-5
L4440 spe-5 dpy-5
mes-4 RNAi dpy-5
L4440 dpy-5

Figure 11

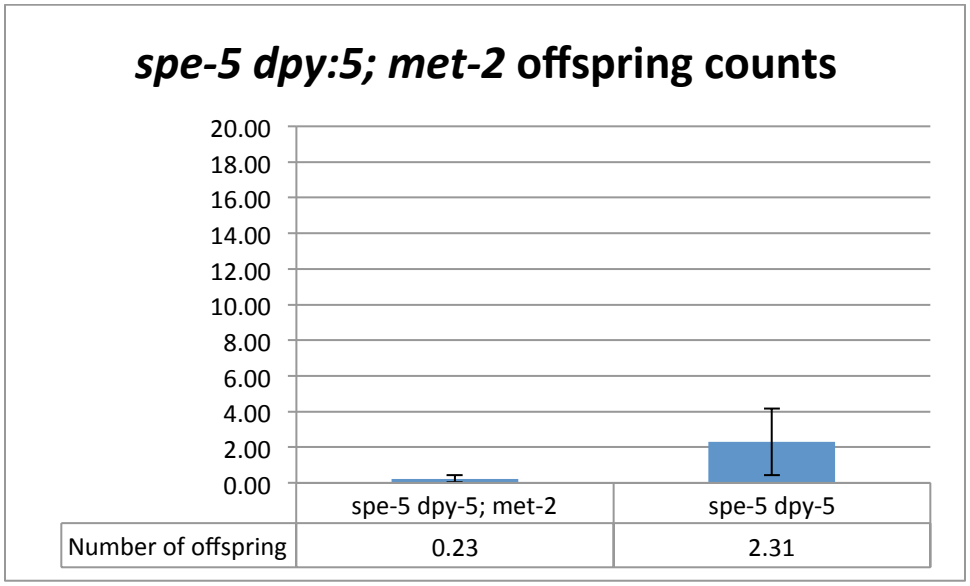

	spe-5 dpy-5; met-2	*spe-5 dpy-5*
Mean offspring	0.23	2.31
Standard Error	0.19	1.88

Figure 12

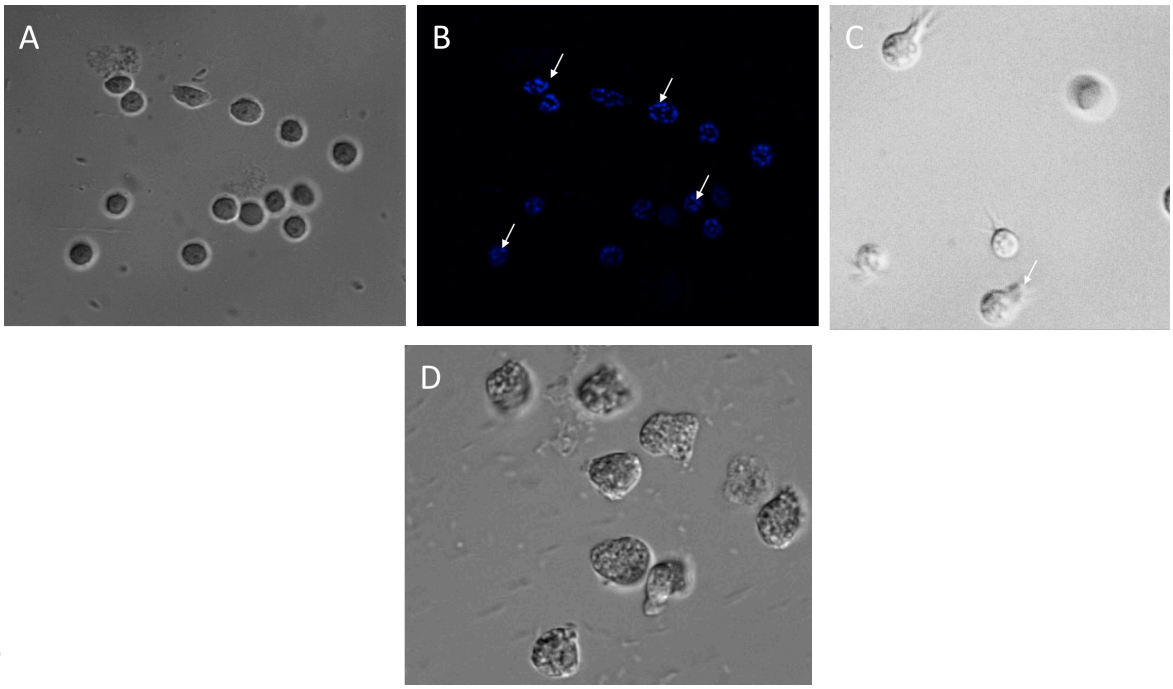

Figure 13

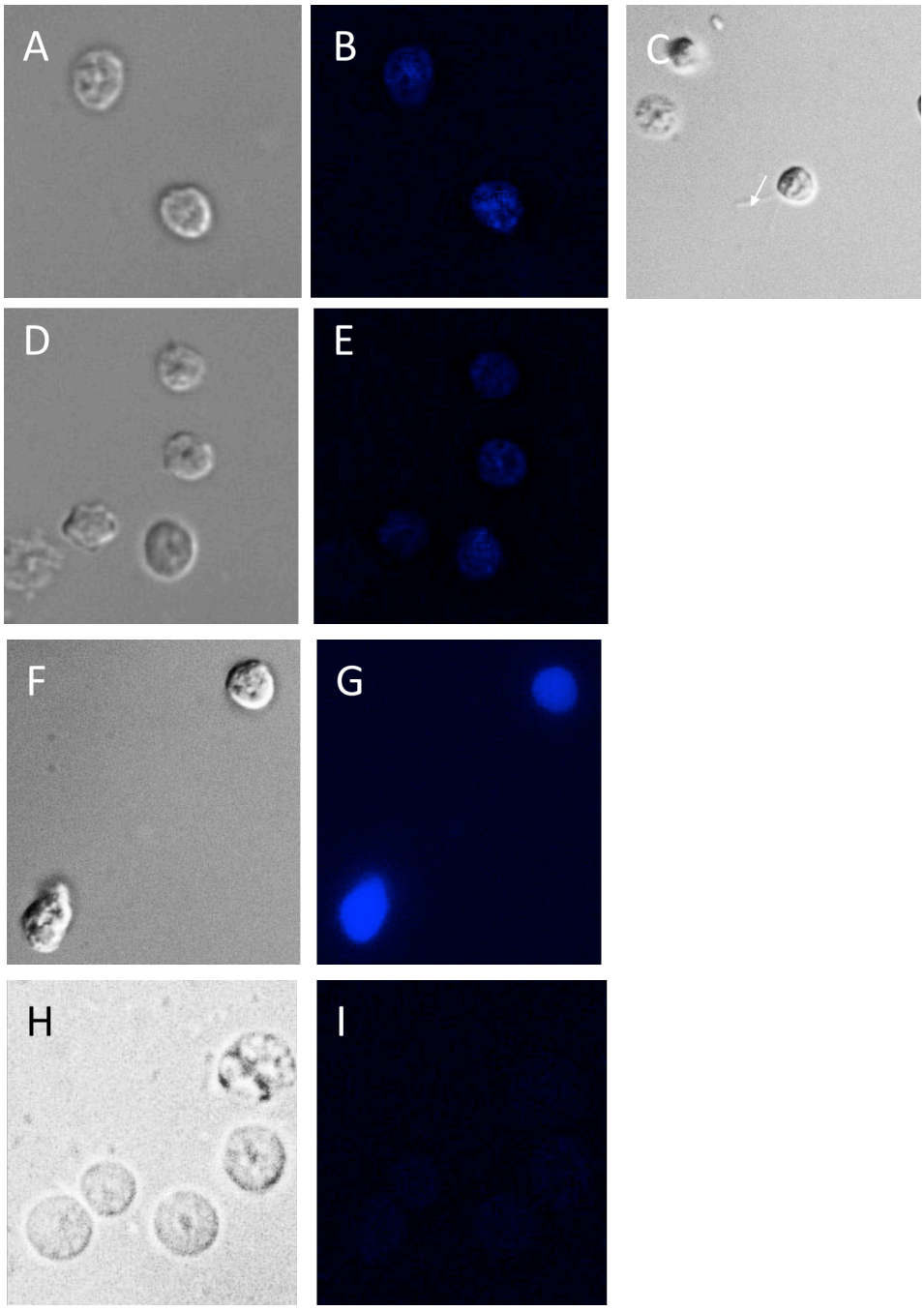

Figure 14

Primer	Sequence	Melting Temperature (°C)
vha-12 upstream sense	5' GGG TTG AAA ATG AGG AAT AAT CGC 3'	54.6°
vha-12 downstream antisense	5' TTA CCT GTC CAC GGG CAA TAG AG 3'	58.5°
vha-12 3' upstream sense	5' GGT AGG CGA GGA ATT CAG CG 3'	58.1°
vha-12 3' downstream antisense	5' GGT AGG CGA GGA ATT CAG CG 3'	56.3°
vha-12 3' LP	5' ATC CAC TAC CAA ACC GTT ACT GAC 3'	60.1°
vha-12 Xma I sense	5' TGC AAT TTT CCC GGG ATG GC 3'	58.9 °
vha-12 Xma I anti-sense	5' GCC ATC CCG GGA AAA TTG CA 3'	58.9°
vha-12 3' *Xma* I sense	5' GGA ATA ACC CGG GTT GGA ATT G 3'	56.2°
vha-12 3' *Xma* I antisense	5' CAA TTC CAA CCC GGG TTA TTC C 3'	56.2°
spe-5 Xma I sense- Failed Primer 1	5' GCG CCC GGG ATG ACA GAA GC 3'	60.0°
spe-5 Xma I antisense- Failed Primer 2	5'CCG CCC CGG GCT ATT GCT TC 3'	60.0°
spe-5 Xma I sense- Higher Tm	5' GCG CCC GGG ATG ACA GAA GCA TCG GAG ATT A 3'	67.3°
spe-5 Xma I antisense- Higher Tm	5'CCG CCC CGG GCT ATT GCT TCT TTC TTT TAT AAT ATT 3'	62.6°

Table 1